8-2003

# Comparison of Bit Error Rate and Power Spectral Density on the Ultra Wideband Impulse Radio Systems

Ömer Sezer
*University of Tennessee - Knoxville*

To the Graduate Council:

I am submitting herewith a thesis written by Ömer Sezer entitled "Comparison of Bit Error Rate and Power Spectral Density on the Ultra Wideband Impulse Radio Systems." I have examined the final electronic copy of this thesis for form and content and recommend that it be accepted in partial fulfillment of the requirements for the degree of Master of Science, with a major in Electrical Engineering.

Mostofa Howlader, Major Professor

We have read this thesis and recommend its acceptance:

Paul B. Crilly, Hairong Qi

Accepted for the Council:
Dixie L. Thompson

Vice Provost and Dean of the Graduate School

(Original signatures are on file with official student records.)

To the Graduate Council:

I am submitting herewith a thesis written by Ömer Sezer entitled "Comparison of Bit Error Rate and Power Spectral Density on the Ultra Wideband Impulse Radio Systems." I have examined the final electronic copy of this thesis for form and content and recommend that it be accepted in partial fulfillment of the requirements for the degree of Master of Science, with a major in Electrical Engineering.

Mostofa Howlader

Major Professor

We have read this thesis and
recommend its acceptance:

Paul B. Crilly

Hairong Qi

Acceptance for the Council:

Anne Mayhew

Vice Provost and Dean of
Graduate Studies

(Original signatures are on file with official student records.)

# COMPARISON OF BIT ERROR RATE AND POWER SPECTRAL DENSITY ON THE ULTRA WIDEBAND IMPULSE RADIO SYSTEMS

A Thesis
Presented for the
Master of Science
Degree
The University of Tennessee, Knoxville

Ömer Sezer
August 2003

**DEDICATION**

This thesis is dedicated to my parents

Mrs. Semra Sezer

and

Mr. Fevzi Sezer

I am very grateful for all the endless love, encouragement, support, and trust they have given me over the years to follow my own path.

## ACKNOWLEDGEMENTS

I would like to thank many people who supported me during my thesis work. I am thankful to my advisor, Dr. Mostofa Howlader, for his supervision, his guidance, and his support. I am thankful to Dr. Paul Crilly not just for being in my committee but also for supporting me since my first day at The University of Tennessee. I am also thankful to Dr. Hairong Qi for being on my committee and her understanding and support during the class work of my first semester.

I thank the Wireless Communication Research Group (WCRG) students for both tough and fun times we spent together.

I would also like to thank in a special way to Burak Özpineci for his support, his guidance, his friendship, and most importantly his brotherhood.

I would like to acknowledge my grandmother, Fadime Sezer, who passed away on November 2002. Even though she is far away, I still feel her presence and support as she is here.

I would like to thank my grandmother, Vahide Abacı for her love and prayers; my aunt, Özden Cıldır for her love and support; my aunt, Nevin Abacı for her love and encouragement; my uncle, Yaşar Abacı for his advice on life; my uncle, Murat Abacı for his brotherhood and friendship; and Ilker Özkaya for being my best friend.

I would like to thank a very special person, my brother, Orkun Sezer, for always being around to fight with, talk with, and for always being extremely happy and thoughtful.

Finally, I am very grateful to my fiancée, my wife to be, Özge, for believing in my abilities and encouraging me to pursue this goal. None of this would have been possible without her continued and endless love and support.

## ABSTRACT

Ultra-Wideband (UWB) is defined as a wireless transmission scheme that occupies a bandwidth of more than 25% of its center frequency. UWB Impulse Radio (UWB-IR) is a popular implementation of the UWB technology. In UWB-IR, information is encoded in baseband without any carrier modulation. Pulse shaping and baseband modulation scheme are two of the determinants on the performance of the UWB-IR.

In this thesis, both temporal and spectral characteristics of the UWB-IR are examined because all radio signals exist in both the time and frequency domains. Firstly, the bit error rate (BER) performance of the UWB-IR is investigated via simulation using three modulation schemes: Pulse position modulation (PPM), on-off shift keying (OOK), and binary phase shift keying (BPSK). The results are verified for three different pulse shaping named Gaussian first derivative, Gaussian second derivative, and return-to-zero (RZ) Manchester. Secondly, the effects of the UWB-IR parameters on the power spectral density (PSD) are investigated because PSD provides information on how the power is distributed over the radio frequency (RF) spectrum and determines the interference of UWB-IR and the existing systems to each other in the spectrum. The investigated UWB-IR parameters include pulse duration, pulse repetition rate, modulation scheme, and pseudorandom codes.

## TABLE OF CONTENTS

## LIST OF FIGURES

# CHAPTER 1
# INTRODUCTION

Today, many wireless technologies exist for different communications needs. There are systems transmitting signals at low data rates to long-range distances, higher data rates to mid-range distance, and high data rates to shorter-range distances. What is missing is achieving extremely high data rates in very short-range distances. The radio spectrum, however, is limited and is getting more crowded due to the increasing demand for radio and wireless communications. UWB may fulfill the communications' need for extremely high data rate in short-range distances due to its ability to share the spectrum with the existing users without interfering with them.

## 1.1 What is UWB?

UWB is defined as a wireless transmission scheme that occupies a bandwidth of more than 25% of its center frequency. UWB uses baseband transmission without carrier modulation. Thus, UWB does not suffer from problems including sensitivity to multipath propagation like the carrier-based modulation systems do. UWB may also be called impulse radio, impulse radar, time-domain, nonsinusoidal, baseband, carrierless, carrier-free, ultra high resolution, and etc.

UWB is different from the narrowband and other wideband systems in two aspects [1]. Firstly, the bandwidth of this technology is more than 25% of a center frequency. Obviously, this bandwidth is much greater than any bandwidth used by any current technology for communications. Secondly, UWB is implemented in baseband. In other words, information is encoded in a baseband signal and carrier modulation is not required while traditional wideband and narrowband systems use RF carriers to move the information in the frequency domain from baseband to the actual carrier frequency.

UWB is a wireless technology utilized in transmitting digital data over a wide spectrum of frequency bands with very low power for communication applications, in carrying signals through doors and other obstacles for radar applications; and in resulting

precise measurements for tracking applications. Several benefits of this technology include excellent immunity to interference and multipath, simple and low cost circuit, low power consumption, high channelization, and the ability to provide high data-rate links.

UWB technology has potential for transmitting large data rates at very low PSDs over short distances, which makes it a candidate for short-range communication applications. Due to the extremely short duration of the pulses, UWB signals are immune to the multipath effects that existing wireless systems suffer. UWB signals are radiated in two methods: UWB-IR and Direct Sequence Phase Coded UWB (DSC-UWB). UWB-IR uses low duty cycles, while DSC-UWB uses high duty cycle. Even though both methods create a wide spectrum in frequency domain, the transceiver techniques, propagation characteristics, and applications for each method are different. UWB-IR, a popular implementation of the UWB technology, is the focus of this thesis.

UWB-IR systems communicate with a series of very short duration pulses called monopulses, where pulse durations are on the order of nanoseconds. These narrow pulses spread the energy of the signal from near dc to a few GHz, which make the signal UWB. Monopulses are uniformly spaced apart in time about a hundred to a thousand times the pulse duration, which make pulse train low-duty-cycle. The lower the duty cycle, the lower power UWB-IR consumes. Equally spaced monopulses does not carry any information itself.

UWB-IR operates in range, which is a densely crowded frequency range [2]. There are narrowband radios operating in the same band, and a UWB-IR scheme causes interference to those. To overcome this interference, UWB-IR uses time hopping techniques. Each user is assigned a pulse pattern, which is referred as time hopping code. The signal is not detectable even if the receiver is very close to the transmitter unless the receiver owns the same time hopping code. In other words, only receiver with the same code can decode the transmitted signal. Time hopping code is to reduce the PSD of the uniformly spaced pulse train. As a result, UWB-IR does not interfere with the narrowband radios.

Additional processing is necessary to modulate the monopulse train in order to transmit information. Information is transmitted at the rate of many pulses per data bit. The modulation has an impact on smoothing the PSD of the signal. This makes the system less likely to interfere with the existing narrowband and wideband signals.

The receiver for an UWB-IR system needs to recognize the time-hopping code sequence in order to decode the transmitted signals. The receiver for a single user using UWB communications is a pulse correlation receiver [3]. A correlation receiver multiplies the received RF signal out of the receiver antenna with the template pulse, then integrates the output, and gets a single dc value. This process occurs over the duration of the pulse. The receiver finally decides on the transmitted data by comparing the dc value with the threshold value.

In UWB-IR, the pulse shape determines the performance of the entire system, which makes it the most important element. It determines the signal's power spectrum and its interference with the other systems. The pulse shape contributes to the output of the receiver as well.

## 1.2 UWB-IR and Spread Spectrum Techniques

UWB-IR may be confused with Spread Spectrum (SS) techniques. SS systems have a transmitted signal that is spread over a frequency band much wider than the minimum bandwidth required to transmit the information being sent [4]. SS system take a baseband signal with a few kHz bandwidth and modulates it with a wideband encoding signal. The encoding signal distributes the baseband signal over a larger bandwidth. The resulting signal might be 1 MHz modulation signal on a several hundred MHz carrier signal with a fractional bandwidth near 1%. Even though SS signals have a wider bandwidth compared to the other signals, they do not fit the UWB definition since their fractional bandwidth is below 25%.

Direct-Sequence Spread Spectrum (DSSS) and Frequency-Hop Spread-Spectrum (FHSS) are two typical spread spectrum techniques. DSSS is similar to FM because the modulation scheme causes the transmitted message's frequency content to be spread out over the spectrum. In FM, the spectrum spreading is obtained by the message. However,

in DSSS, a pseudorandom number generator causes the spreading. In FHSS, the carrier frequencies of the individual users are varied by pseudorandom number (PN) sequence. PN generator drives a frequency synthesizer that produces a wideband sequence of frequencies. The synthesizer causes the data modulated carrier to hop from one frequency to another.

The main difference between the SS and UWB-IR systems is that the wide bandwidth in a UWB-IR waveform is produced by pulse duration and pulse shaping, and not by spreading with a chipping or hoping sequence as it is in DSSS or FHSS. The wide bandwidth for a UWB-IR pulse is generated directly by the properties of the Fourier transforms relationship between time and frequency. Short pulse directly generates a wide bandwidth signal in this time-domain concept. In addition, SS waveforms are constant envelope, which means that the waveforms have unity duty cycle, while UWB-IR pulses typically have very small duty cycle.

## 1.3 Features of UWB-IR

UWB-IR can be characterized by:

- Ultra-short duration pulses that yield ultra-wide bandwidth signals
- Transmission with very low power (few analog components and low duty cycle signal)
- Excellent immunity to interference from other radio systems
- No interference with existing spectrum users (because UWB signals are buried in the noise)
- No allocated spectrum necessary
- Penetration capability through the walls and ground (low frequency component of UWB technology)
- High precision ranging (high frequency component of UWB technology)
- Wide bandwidth results in the ability to resolve multiple paths and reduce multi-path interference
- Simple and inexpensive circuit

## 1.4 UWB Applications

The characteristics of UWB makes it an alternative technology for the applications such as high precision positioning and tracking systems, high-speed local area networks (LANs), personal area networks (PANs), collision avoidance sensors, in-building personnel and asset tracking, through wall motion detection and tracking, home networks, and invisible security domes and fences. UWB is becoming more and more attractive in radar, communications, and geolocation applications.

Radar applications include vehicular radar, ground penetrating radar (GPR), through wall imaging radar, medical imaging radar, security systems tracking movement, collision avoidance sensors for cars and boats, industrial robotic controls, and advanced highway construction and inspection equipment.

Communications applications include LANs, PANs, short-range radios, military communications, in-building communications systems, and wireless broadband Internet access.

Precision geolocation is another UWB application. UWB can be used to measure distance in a method similar to the one in Global Positioning Satellite System (GPS). GPS uses satellites to transmit radio signals carrying timing information. The GPS receiver communicates with multiple satellites and calculates its location by comparing the different timing signals. Therefore, it is a good technique for outdoor applications. However, applying this technique to heavily shadowed and covered urban environments is difficult and impossible for indoor applications. Since the UWB system works well in multi-path and inside the buildings, it is an excellent technique for high precision, indoor positioning applications.

## 1.5 Outline of the Thesis

The objective of this study is to investigate the temporal and spectral characteristics of the UWB-IR signals. The effects of some UWB-IR parameters on the BER, and PSD of a UWB-IR system are analyzed in the following order.

Chapter 2 begins with the summary of UWB technology history and continues with the regulations of this technology. Following are the explanations of UWB

definition, processing gain, and capacity. The chapter concludes with the overview on previous and current researches on the topic.

Chapter 3 gives a system model of the transmitter and receiver of a UWB-IR system.

Chapter 4 presents three pulse shapes and three modulation scheme candidates used in simulations for UWB-IR systems. The chapter discusses the simulation results for BER comparison in Additive White Gaussian Noise (AWGN) channel only and Rayleigh fading channels. Following, the effects of UWB-IR parameters such as pulse duration, pulse repetition rate, modulation scheme, and pseudorandom code on the PSD of UWB-IR systems are analyzed.

Chapter 5 provides conclusion and overall summary of this thesis.

# CHAPTER 2
# LITERATURE SURVEY

In the previous chapter, the features and applications of UWB technology are summarized. It is necessary to have a good understanding of UWB technology before studying the system model and research. In this chapter, history of UWB technology is given first. Following is the regulation of UWB technology. Then, a capacity definition for UWB and its comparison with the current wireless standards are presented. Finally, a summary of what has been done in UWB research so far and the current research are explained.

## 2.1 History of UWB

The origin of UWB technology begun in 1962 by describing the transient behavior of a microwave network through their characteristic impulse response [5]. In 1968, impulse measurement techniques were applied to the design of wideband, radiating antenna elements. During the same period, it was found that short pulse radar and communications systems could be developed with the same set of tools. Different techniques were applied to various applications in radar and communications. The invention of a short pulse receiver to replace the time-domain sampling oscilloscope sped up the system development. This was awarded as the first UWB communications patent. Through the late 1980's, this technology was referred to as *baseband*, *carrier-free* or *impulse*. The term "ultra-wideband" was applied first time in 1989 by the U.S. Department of Defense (DoD) after nearly thirty years of development in theory, techniques, and hardware approaches. In 1989, many patents were awarded in UWB pulse generation and reception methods and applications such as communications, radar, automobile collision avoidance, positioning systems, liquid level sensing, and altimetry. In the United States, much of the research in UWB was done before 1994 in the area of impulse communications performed under U.S. Government programs. Since 1994, the

research has been done without any restriction for classification. The development of UWB technology has been growing rapidly since then.

## 2.2 Regulations for UWB

In the United States, Federal Communication Commission (FCC) and National Telecommunications and Information Administration (NTIA) together manage the radio spectrum allocation. Because UWB is a RF technology, it can interfere with the existing licensed systems in the frequency spectrum. Therefore, UWB needs to be regulated.

The FCC has stated the importance of UWB technology after receiving requests. The FCC started the review process in 1998. Two years later, the FCC released a Notice of Proposed Rulemaking (NPRM) accepting comments and feedback from the industry. Finally, on February 14, 2002, the FCC approved the limited uses of UWB after receiving comments and review from the FCC, NTIA, Department of Commerce, and DOD. UWB is restricted to intentional operation only from 3.1 to 10.6 GHz for communication devices; from 1.99 to 10.6 GHz for through-wall imaging and surveillance systems; and above 24.075 GHz for automotive radars. The reason for limiting the uses of UWB is to make sure that UWB radiations will not disturb or interfere with any of the systems on the licensed bands, especially safety-of-flight and safety-of-life such as Global Positioning System (GPS). The factors affecting the UWB interference with the existing systems are studied in detail in Chapter 4. UWB emissions are to be lower than the limit for unintentional radiators that radiate signals in licensed bands is in Part 15 of Volume 47 of the Code of Federal Regulations. The limit is the measured electric field strength of 500 microwatts per meter at a distance of 3 meters in a 1MHz bandwidth for frequencies above 960 MHz, which corresponds to an emitted PSD of –41.3 dBm/MHz [1].

## 2.3 UWB Definitions

Although many definitions exist, there are still no widespread standards for UWB technology. FCC defines UWB as a technology, whose bandwidth is more than 25% of a center frequency or more than 500 MHz. The Defense Advanced Research Project

Agency's (DARPA) 1990 *Assessment of Ultra-Wideband Radar* advised that "definitions need liberal interpretation and that mathematical definitions are difficult to achieve and seldom useful in practical sense." The following definitions were given in [6].

Energy Bandwidth, $B_E$: The energy bandwidth is the frequency range within which some specified fraction, say 90 or 99%, of the total energy lies. This must be defined for a single pulse, if all pulses are the same, or for a group of pulses that are processed together to yield a single decision. The upper limit of this range is denoted here by $f_H$ and the lower limit by $f_L$.

Time-Bandwidth Product, TB: The time-bandwidth product of a signal is defined as the product of the energy bandwidth and the effective duration of a single pulse or pulse group. It is the measure of the increase in peak signal-to-noise ratio (SNR) that can be achieved in the radar receiver by appropriate signal processing.

Bandwidth can defined as fractional bandwidth (FB) and relative bandwidth (RB):

$$FB = \frac{2(f_H - f_L)}{(f_H + f_L)}, \tag{2.1}$$

$$RB = \frac{(f_H - f_L)}{(f_H + f_L)}, \tag{2.2}$$

where, $f_H$ and $f_L$ are upper and lower 3dB points of the signal spectrum. The DARPA panel accepted the following definition:

"Ultra-wideband radar is any radar whose fractional bandwidth is greater than 0.25, regardless of the center frequency or the signal time-bandwidth product." [6]

Narrowband refers to electromagnetic signal waveforms that have instantaneous fractional bandwidths less than 1% with respect to a center frequency and wideband from 1% to 25%.

The term ultra-wideband refers to electromagnetic signal waveforms that have instantaneous fractional bandwidths greater than 0.25 with respect to a center frequency.

## 2.4 Processing Gain for UWB

In a SS system, processing gain is the measure of a radio's resistance to jamming [4]. This can be calculated as the ratio of the transmitted signal bandwidth to the information bandwidth. However, for a UWB system, the processing gain cannot be calculated the same way. The processing gain for a UWB system is defined in [4] as:

$$N_s = \frac{P}{P_{ave}} = \frac{B}{R}, \tag{2.3}$$

where, P is the peak power, $P_{ave}$ is the average power, B is the occupied bandwidth of the waveform, and R is the data rate or pulse repetition frequency. For a fixed average power, when the data-rate is decreased, the peak power increases. Therefore the signal becomes easier to detect in noise. However, this cannot be called "processing-gain" because an increase in the peak-power is required to achieve the gain. UWB systems are peak-power limited and their performance is determined by the received SNR as:

$$SNR = \frac{E_b}{N_0}, \tag{2.4}$$

where, $E_b$ is the energy per bit, and $N_0$ is the noise spectral density. $N_0$ can be expressed as:

$$N_0 = kT_eB, \tag{2.5}$$

where, k is Boltzmann constant, $T_e$ is system noise temperature, and B is the bandwidth. It is important to note that the noise spectral density depends on the bandwidth, thus more energy is needed for a wider bandwidth.

Energy per bit for a UWB technology can be defined as:

$$E_b = PT\,, \tag{2.6}$$

where, T is the pulse duration. From (2.6), for a given BER, higher peak power is needed for a shorter UWB pulse.

For SS systems, a doubling of the data rate requires a doubling of the peak and average power [4]. However, this is not the case for a UWB system. *In a UWB system, energy per bit does not depend on the data rate.* In other words, since the pulse duration is fixed, when the data rate needs to be doubled, there is no need to double the peak power in order to keep the product in (2.6) a constant. The peak power is adjusted for the required BER. The average power, on the other hand, depends on the data rate. Higher data rates require higher average powers, therefore higher duty cycles.

UWB systems have many advantages over SS systems. One advantage is that, in terms of BER performance, UWB is independent of any changes in data rate. UWB's simple and low cost implementation for high data rates is another advantage over SS.

## 2.5 Capacity for UWB

The spatial capacity is measured as the average data rate per coverage area. The unit of spatial capacity is bits per second per square-meter because the coverage area is two-dimensional. Following are the spatial capacity of UWB and its comparison with the current short and medium range wireless standards, such as IEEE 802.11a-b, and Bluetooth as in [1].

IEEE 802.11b systems use 80MHz spectrum in 2.4GHz band. Three 22MHz IEEE 802.11b systems can operate without interfering each other in a circle with the radius of 100m. Each system has a peak speed of 11 Mbps. The total data rate is 3x11Mbps, or 33Mbps. The coverage area is the area of the circle, $\pi(100)^2$, or $10{,}000\pi$. Therefore the spatial capacity is 33Mbps/$10{,}000\pi$, or 1,000 bps/$m^2$.

IEEE 802.11a systems use 200MHz spectrum in 5GHz band. Twelve systems can operate in a circle with the radius of 50m. Each system has a peak speed of 54 Mbps. The

total data rate is 12x54Mbps, or 648Mbps. The coverage area is the area of the circle, $\pi(50)^2$, or 2,500π. Therefore the spatial capacity is 648Mbps/2,500π, or 83,000 bps/$m^2$.

Bluetooth is another standard, where ten of them can operate in a circle with the radius of 10m. Each system has a peak speed of 1Mbps. The total data rate is 10x1Mbps, or 10Mbps. The coverage area is the area of the circle, $\pi(10)^2$, or 100π. Therefore the spatial capacity is 10Mbps/100π, or 30,000 bps/$m^2$.

In UWB, six systems can operate in a circle with the radius of 10m. Each system has a peak speed of 50Mbps. The total data rate is 6x50Mbps, or 300Mbps. The coverage area is the area of the circle, $\pi(10)^2$, or 100π. Therefore the spatial capacity is 300Mbps/100π, or 1,000,000 bps/$m^2$.

Table 2.1 shows the comparison of the wireless standards and UWB. None of the current wireless standards reach the capacity of UWB presented in Table 2.1. The reason lies on the channel capacity theorem, which is defined in [1] as:

$$C = B\log_2(1+\frac{S}{N}), \tag{2.7}$$

where, C is the maximum channel capacity, B is the channel bandwidth, S is the signal power, and N is the noise power. As seen in (2.7), capacity is linearly proportional with bandwidth and logarithmically with signal to noise ratio. As presented in Table 2.1,

Table 2.1: Comparison of wireless standards and UWB.

| | **Operating Range (m)** | **Data Rate (Mbps)** | **Spatial Capacity (kbps/$m^2$)** |
|---|---|---|---|
| IEEE 802.11b | 100 | 33 | 1 |
| IEEE 802.11a | 50 | 648 | 83 |
| Bluetooth | 10 | 10 | 30 |
| UWB | 10 | 300 | 1,000 |

UWB gives the highest capacity because UWB occupies much wider bandwidth than any other technology.

## 2.6 Research

More and more papers have been published in UWB communications systems. There are many papers that have focused on different aspects of the UWB technology including regulations, electromagnetics, communications, channel measurement and models, interference, multipath fading, multiple access systems, antenna, hardware, radar, and other applications.

The first paper that received great attention was [3], where for the first time, the features of UWB-IR using a binary PPM scheme was presented, an estimate of the multiple access capability of a communication system employing this format under ideal propagation conditions was given, and the design issues were described. Four years later, in 1997, [7] studied the performance of the same system in [3], including the estimate of the multiple access capability for analog modulation format as well as digital format. Same authors expanded their studies by presenting time hopping sequence design in [8] and by estimating the system's performance in terms of achievable transmission rate in [9]. In [10], the paper analyzes the performance of UWB-IR by employing block waveform PPM modulation. [11] analyzes the same system in [10] by investigating multiple access performance of different M-ary PPM signal designs in free space propagation conditions in terms of the number of users supported by the system for a given BER, SNR, bit transmission rate, and number of signals in the M-ary set. The number of the publications on UWB-IR has been increasing rapidly since then.

UWB communication systems have been proposed for use in dense multipath or shadowed environments. Enormous number of papers concentrated on the evaluation of propagation and multipath characteristics of the UWB-IR communication channels as well as the Rake receivers as in [12]-[14]. [15] proposes and studied a new algorithm for the UWB channel characterization in detail. In [16], the performance of UWB signals using M-ary PPM scheme in an environment with only AWGN versus with dense multipath environment with AWGN is compared in order to evaluate the fading margin.

The same paper shows that the presence of multipath causes small increase in SNR required to achieve reasonable levels of BER and this small fading margin can be understood by the ability of the UWB signal to resolve the dense multipath. In [17], the performance of non-binary UWB-IR modulation in the presence of AWGN only and multipath with AWGN channels is investigated with detection using a Rake receiver. [18] investigates the multipath characteristics of UWB-IR by observing the characteristics of BERs through computer simulations for the deterministic two-path model and the statistical indoor multipath model of Saleh and Valenzuela. In [19], the paper presents a differential detector that rakes in some multipath energy, while relaxing some of the implementation requirements. The same paper also analyzes the performance and the implementation of the differential detector, and compares it to a rake receiver with a correlation receiver detector in the presence of AWGN and multipath.

UWB-IR signal design in multipath environment is another interest among these papers. [20] describes the construction of equally correlated PPM signals using trains of UWB pulses and analyzes the performance of these signals in indoor UWB-IR channel with detection using a rake receiver. In [21], the paper investigates communications using quaternary PPM over the indoor multiple access channel with multipath and the performance of these signal sets with different correlation properties.

On the other hand, some papers also analyze the experimental results of UWB-IR channels rather than only analytical results. [22] describes both analytical and experimental analyses to quantify the tradeoff between energy capture and diversity level in Rake receiver using measured received waveforms obtained from UWB signal propagation experiments. In [23], the paper presents the results of a UWB signal propagation experiment performed in a typical modern office building, which show that UWB signals do not suffer multipath fading. [24] explores some of the propagation characteristics associated with UWB signals based on measured data.

The interference of narrowband and wideband communication systems with UWB communications was another focus in the published papers. In [25], the performance of UWB communications in the presence of interference is analyzed. In addition, a comparison between the interference capabilities of UWB and DSSS is made

and it is shown that the jam suppression of UWB is superior to that of DSSS. [26] quantifies the effect that a UWB interferer has on bit error probability of a narrowband system in order to determine the applicability of the white, Gaussian noise. In [27], the paper illustrates the nature of the multiple access interference and the application of multi-user detection to improve the performance of UWB-IR system. [28] provides the performance of UWB communications in the presence of single tone, continuous wave jamming and multi-tone jamming or interference as well as the analytical results for pulse shaping and correlation receivers.

There are several papers published ([1],[29]-[33]) that focus on the modulation scheme and PSD of UWB-IR technology, which is the concentration of this thesis. In [1], the paper quantifies the distance versus throughput relationship for M-ary Pulse Amplitude Modulation (PAM) system in order to highlight some of the advantages and constraints of UWB-IR. In [29], several candidate monopulse shapes including Gaussian, Gaussian first derivative, Gaussian second derivative, Manchester, RZ-Manchester, sinusoidal, and rectangular monopulses are investigated. Their spectrum characteristics and BER performances in AWGN using only PPM scheme are simulated and compared. Their performances in fading multipath channel are investigated as well. [30] describes PAM and PPM schemes, and coding schemes for UWB-IR systems. The paper also gives mathematical equations and expressions for modulation schemes and their PSDs, and compares them. In [31], the paper presents a new pulse shape that satisfies the FCC requirements. The paper includes mathematical expressions for the PSD of the transmitted signals as well. In [32], the paper describes how a large fractional bandwidth leads to lower fading in the presence of multipath for UWB communication systems. The paper includes expressions for the PSD of the transmitted signals and measurements using an actual UWB communications system showing the magnitude of signal strength variations due to multipath interference. In [33], the mathematical models for describing two modulation schemes, biphase modulation (BPM) and hybrid modulation, which combines BPM and PPM together, are reviewed. A period extension method, which obtains considerable reduction in PSD level, and two implementations for PN sequence in the impulse train used to generate UWB signals are proposed.

This thesis compares the BER performances of PPM, OOK, and BPSK modulation schemes using three different pulse shapes: Gaussian first derivative, Gaussian second derivative, and RZ-Manchester monopulses. Following, the effects of UWB-IR factors including pulse duration, pulse repetition rate, modulation scheme, and pseudorandom codes on the PSD of the transmitted signals are analyzed. In this study, both BER and PSD comparisons are demonstrated in detail with explanations and figures.

# CHAPTER 3
# SYSTEM MODEL

In Chapter 2, the basic concept of UWB-IR technology was explained by its definitions, capacity comparisons with different standards, and processing gain. In this chapter, the system model based on [3] for UWB-IR including the transmitter and the receiver used in simulations presented in detail.

## 3.1 Transmitter

A UWB pulse train signal is represented as a sum of pulses shifted in time in [32] as:

$$s(t) = \sum_j a_j w(t - t_j), \tag{3.1}$$

where, s(t) is the modulated UWB signal, w(t) is the transmitted UWB pulse shape, $a_j$ is the amplitude offset and $t_j$ is the time offset. Figure 3.1 shows Gaussian first derivative pulse, one of the monopulse candidates for UWB. The mathematical expressions and details for this monopulse and two other monopulse candidates are studied in Chapter 4.

From (3.1), a general equation of a modulated UWB signal for every modulation scheme can be written as:

$$s(t) = \sum_j a_j w(t - jT_f - c_j T_c - \delta d_j), \tag{3.2}$$

where, $t_j = jT_f + c_jT_c + \delta d_j$, $T_f$ is the pulse repetition time or frame time, $c_j$ is the time hopping code sequence with an additional time shift of $c_jT_c$ to the $j^{th}$ pulse, $\delta$ is the modulation factor, d is the binary (0 or 1) bit stream data sequence.

The structure of each component in (3.2) is presented as follows:

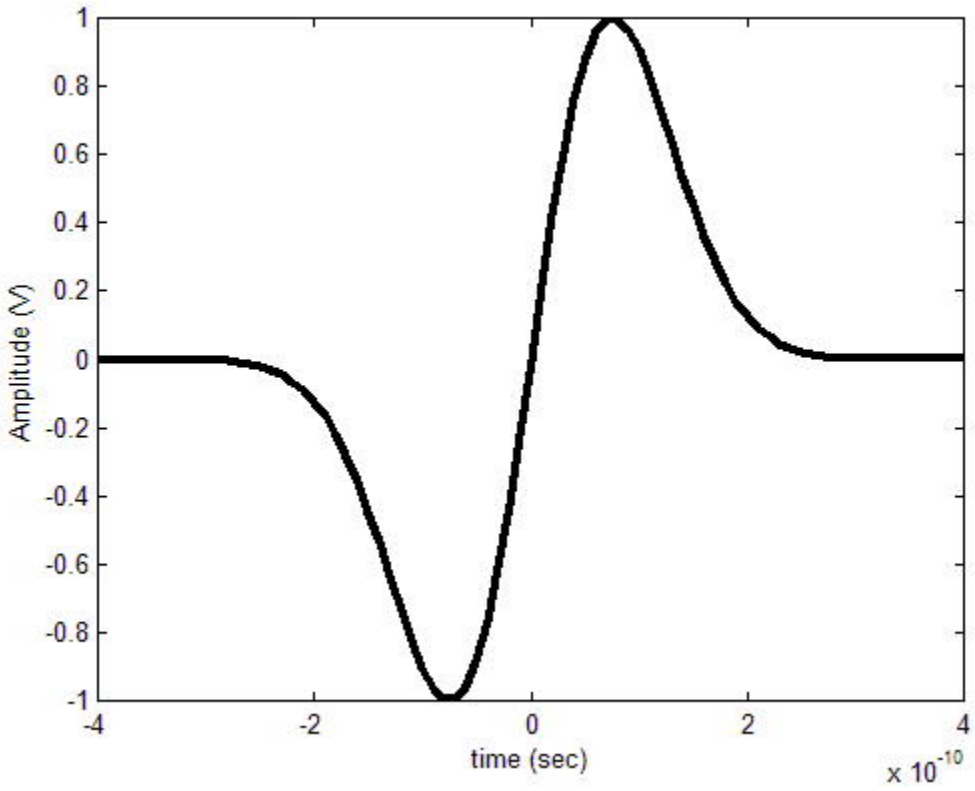


Figure 3.1: Gaussian first derivative pulse in time domain.

### 3.1.1 Uniform Pulse Train Spacing

Time modulation systems use long sequences of monopulses for communications [2]. The pulses are uniformly spaced in time, i.e. $t_j = jT_f$, (3.1) becomes:

$$s(t) = \sum_j a_j w(t - jT_f) . \tag{3.3}$$

(3.3) consists of monopulses spaced $T_f$ seconds apart in time. The frame time, $T_f$, typically may be a hundred to a thousand times the monopulse duration. The result is a signal with a very low duty cycle. Figure 3.2 shows the Gaussian first derivative pulse with duration of 0.6ns within a frame of only 4ns, ($T_f$ = 4ns), for illustration purposes. Figure 3.3 shows the Gaussian first derivative pulse train of 5 monopulses.

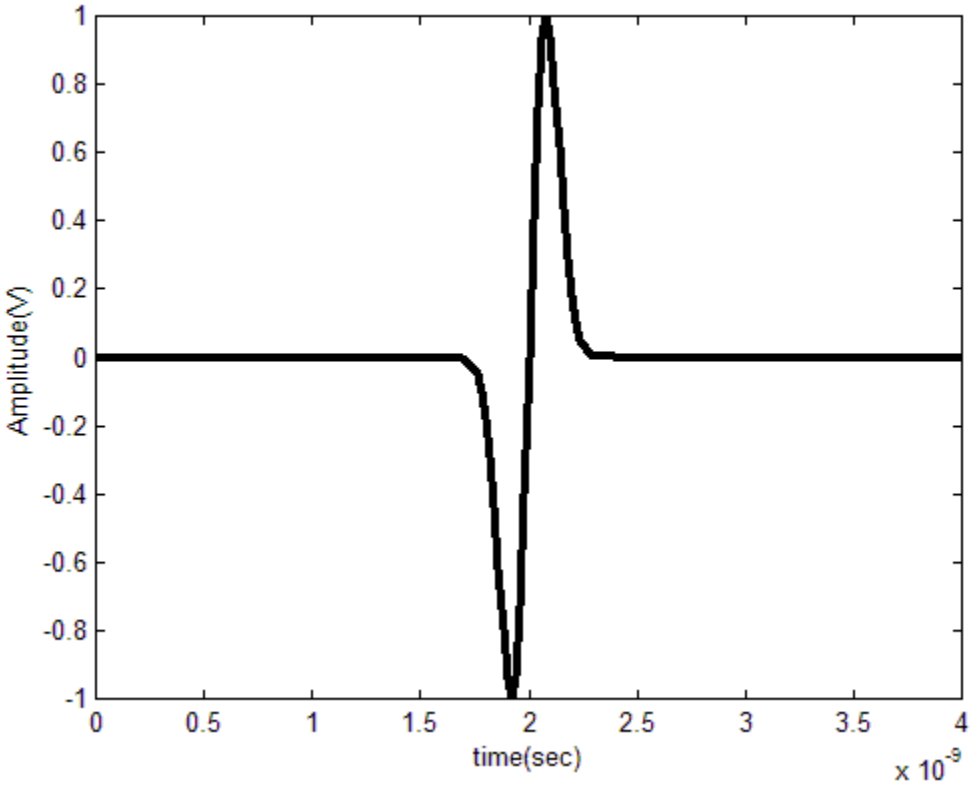


Figure 3.2: Gaussian first derivative pulse within a frame of $T_f$= 4ns.

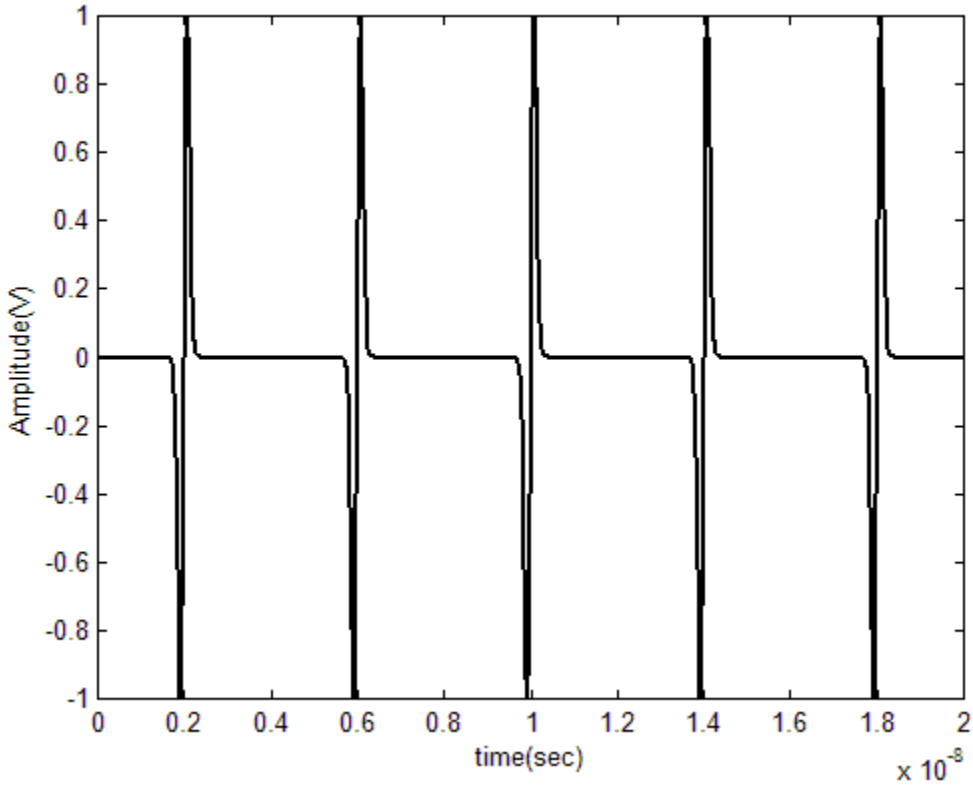


Figure 3.3: Gaussian first derivative pulse train of 5 monopulses.

### 3.1.2 Pseudorandom Time Hopping

Any pulse train at this point does not carry any information and is the same for everybody. The pulse train can be made different for each user by using different pseudorandom codes. The code shifts the time of each transmitted monopulse within the frame. For multiple access purposes, each user has his own code, $\{c_j\}$. This helps eliminating collisions. These codes are periodic pseudorandom codes with period $N_p$. As a result,

$$c_{j+iN_p} = c_j \,, \tag{3.4}$$

for all integers j and i. Each code element is an integer in the range:

$$0 \le c_j \le N_h, \tag{3.5}$$

where, $N_h$ is an integer. The time hopping code, therefore, provides an additional time shift to each pulse in the pulse train. Thus, $j^{th}$ monopulse gets shifted by $c_j T_c$ seconds. Time shifts by the code are discrete times between *0 and* $N_h T_c$ seconds.
It is assumed that:

$$N_h T_c \le T_f. \tag{3.6}$$

The ratio $N_h T_c/T_f$ gives the fraction of the frame time $T_f$ over which time hopping is allowed. Because a short time interval is required to read the output of a monopulse correlator and to reset the correlator, it is assumed that $N_h T_c/T_f$ is strictly less than one. If $N_h T_c$ is too small, then collisions may occur. Because the hopping code is periodic with period $N_p$, the waveform

$$\sum_j a_j w(t - jT_f - c_j T_c),$$

is periodic with period

$$T_p = N_p T_f.$$

In a multiple access system, each user would have a unique code sequence. Only a receiver operating with the same code sequence can decode the transmission. The signal is virtually undetectable without the knowledge of the unique time-hopping code; even if the receiver is very close to the transmitter.

Figure 3.4 shows the regular and coded Gaussian first derivative pulse trains together. The randomly generated sample code used to show the difference between the regular and coded pulse trains is [8 2 6 3 9].

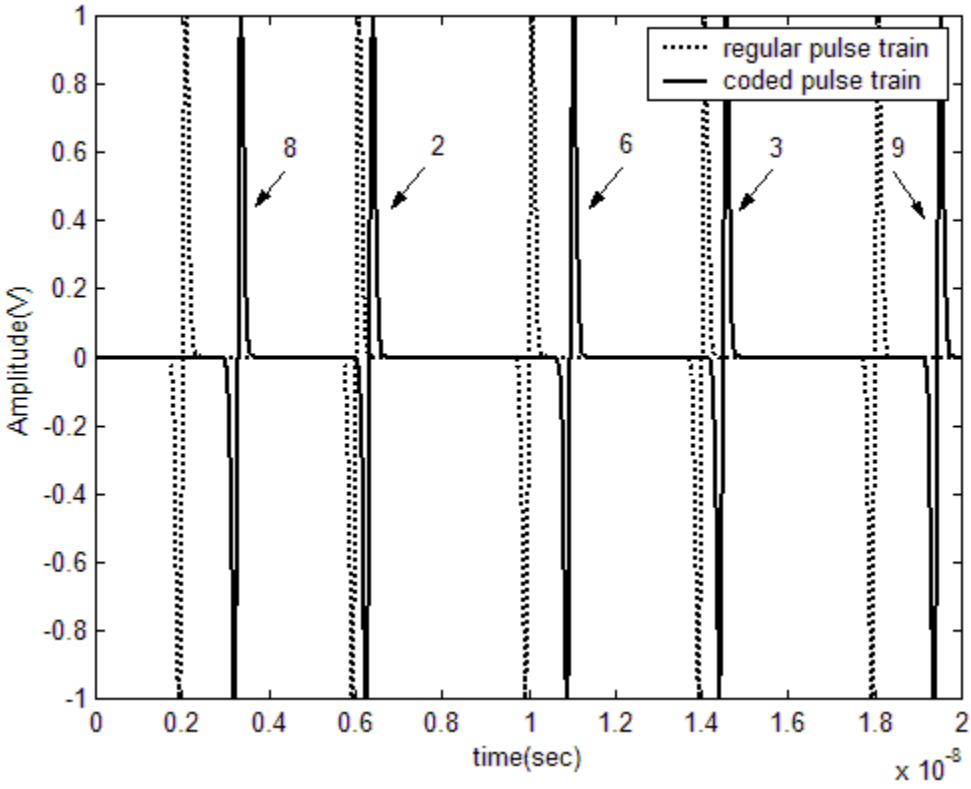


Figure 3.4: Regular and coded [8 2 6 3 9] Gaussian first derivative pulse trains.

### 3.1.3 Data Modulation

In order to transmit information, the pulse train needs to be modulated. The data sequence d of transmitter k is a binary (0 or 1) bit stream. The modulating data bit changes every $N_s$ hops because $N_s$ monopulses are transmitted per bit. A new data bit begins with pulse index j = 0, and the index of data bit modulating pulse j is [j/ $N_s$] [3]. A single bit has duration of:

$$T_s = N_s T_f . \tag{3.7}$$

For a fixed frame $T_f$, the binary bit rate $R_s$ determines the number $N_s$ of monopulses that are modulated by a given binary bit, via the equation:

$$R_s = 1/T_s = 1/N_s T_f . \tag{3.8}$$

The binary bit rate for the signal in Figure 3.3 is $R_s = 1/(2.10^{-8}) = 50$Mbps.

The detailed information and plots of three different modulation schemes for UWB and their effects on the UWB spectrum are studied in Chapter 4. Figure 3.5 is a block diagram of a transmitter for a UWB system.

## 3.2 AWGN Channel

The channel is assumed to corrupt the signal by the addition of white Gaussian noise, as illustrated in Figure 3.6. The composed received signal at the output of the receiver's antenna is given in [3] as:

$$r(t) = As(t-\tau) + n(t), \tag{3.9}$$

where, A is the attenuation of the transmitter signal over the propagation path to the receiver, $\tau$ is the time asynchronisms between the clock of the transmitter and the receiver, and n(t) is the white Gaussian noise with a PSD of

$$\Phi_{nn}(f) = \frac{N_0}{2}. \tag{3.10}$$

The mean of the noise is zero and the variance of the noise is defined in the simulation as:

$$\sigma^2 = \frac{N_0}{2} = \frac{E_b}{2\frac{E_b}{N_0}} = \frac{E_b}{2SNR}, \tag{3.11}$$

where, $E_b$ is defined in (2.6), and SNR is defined in (2.4).

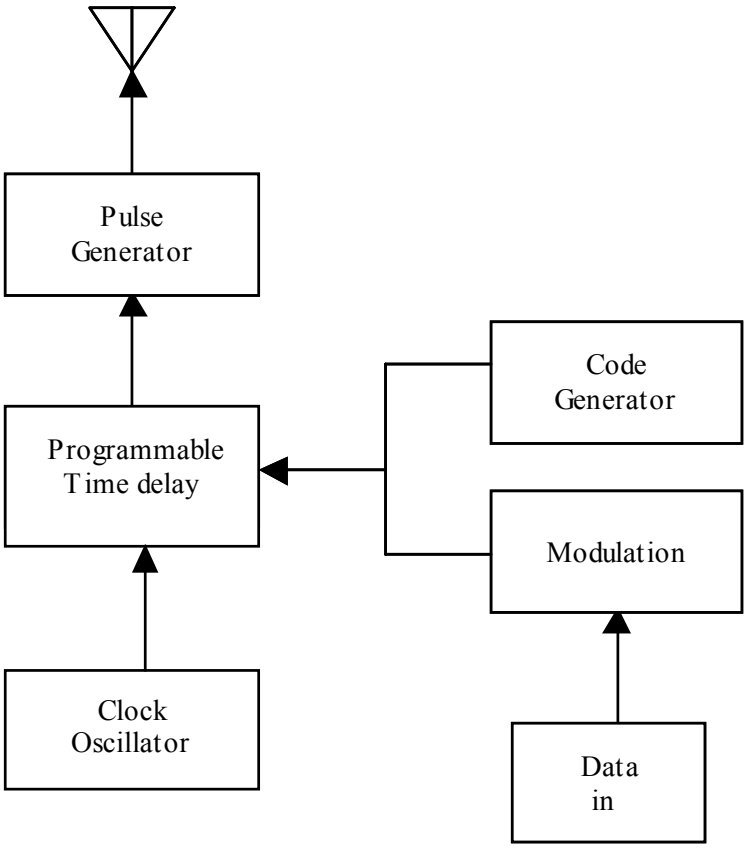


Figure 3.5: Block diagram of the UWB-IR transmitter.

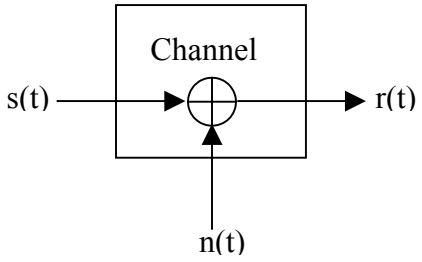


Figure 3.6: The received signal model passed through AWGN channel.

## 3.3 Receiver

The receiver concept for UWB-IR system is based on a hypothesis testing theory in order to detect the data [3]. The received signal is given in (3.9). The receiver must achieve both clock and code synchronization for the signal transmitted. Therefore, the receiver finds out the value of τ, and has a replica of the user's time-hopping code, $c_j$, running synchronously with the time hops received via the air waves from the user.

The receiver must decide on whether the data bit is 0 or 1. The decision is based on the received signal, r(t), in a interval of duration of

$$T_s = N_s T_f . \tag{3.12}$$

The receiver tests the following hypothesis after synchronized to the signal and decides on between hypothesis $H_0$ or $H_1$.

$$H_d : r(t) = A_1 w_{sym}(t - \delta d) + n(t), \tag{3.13}$$

where, d is 0 or 1 and $w_{bit}(t)$ is the bit waveform in this interval and is defined in the receiver as:

$$w_{bit}(t) = \sum_{j=0}^{N_s - 1} w_{rec}(t - jT_f - c_j^{(1)} T_c - \tau) . \tag{3.14}$$

The receiver for this single signal of a binary modulated UWB signal in AWGN is simply a bit duration correlator, a correlation receiver. It is assumed that the data is composed of independent random variables. The correlator correlates the received signal with one-pulse template signal. The template signal, as seen in Figure 3.7, is the difference between the pulse representing bit 0 and the one representing bit 1. The template signal is a reference signal and is defined mathematically as:

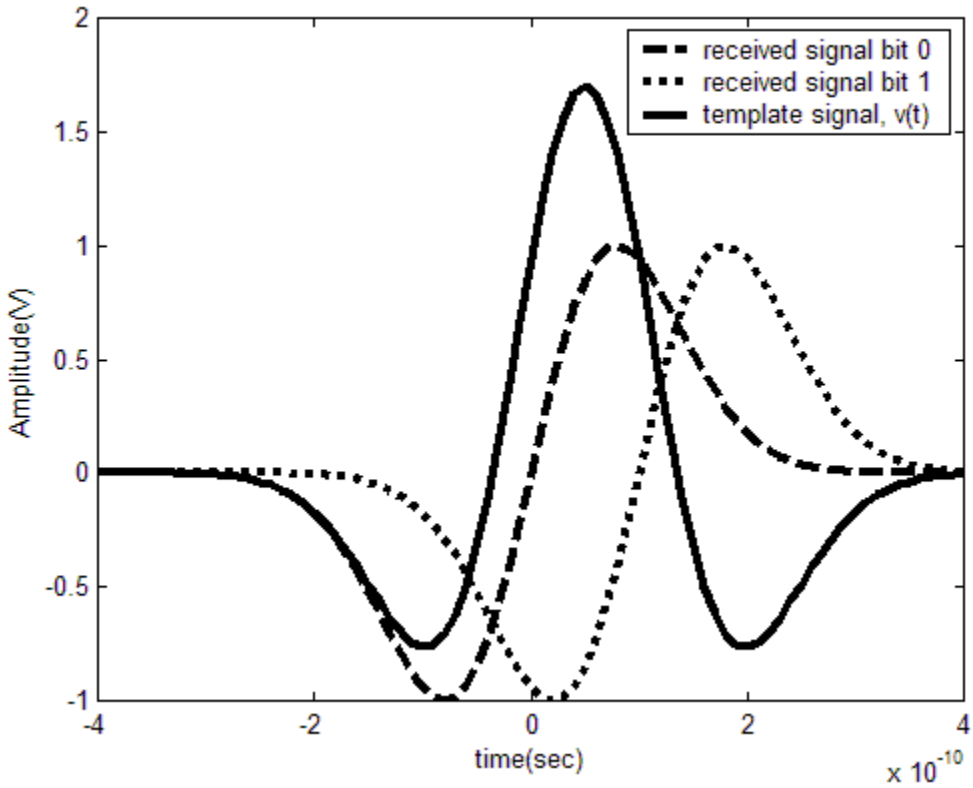


Figure 3.7: Received signal for bit 0 and bit 1 and template signal, v(t).

$$v_{bit}(t) = w_{sym}(t) - w_{sym}(t-\delta), \tag{3.15}$$

$$v_{bit}(t) = \sum_{j=0}^{N_s-1} v_{rec}(t - jT_f - c_j^{(1)} T_c - \tau_1). \tag{3.16}$$

Therefore,

$$v_{rec}(t) = w_{rec}(t) - w_{rec}(t-\delta), \tag{3.17}$$

where, v(t) is nonzero in the interval $[0,T_s]$ since $w_{rec}(t)$ is nonzero in the interval $[0, T_s]$. The decision rule is:

$$\int_{t\varepsilon T_i} r(t)v_{bit}(t)dt \succ 0. \qquad \text{if "H}_0\text{ is true (d=0)"} \tag{3.18}$$

(3.18) can be written as:

$$\sum_{j=0}^{N_s} \int_{\tau_1+jT_f}^{\tau_1+(j+1)T_f} r(t)v(t-\tau_1-jT_f-c_j{}^{(1)}T_c)dt \succ 0 \quad , \quad \text{if "H}_0\text{ is true (d=0)"} \tag{3.19}$$

where,

$$\alpha_j = \int_{\tau_1+jT_f}^{\tau_1+(j+1)T_f} r(t)v(t-\tau_1-jT_f-c_j{}^{(1)}T_c)dt \tag{3.20}$$

is the pulse correlator output and

$$\alpha = \sum_{j=0}^{N_s-1} \alpha_j = \sum_{j=0}^{N_s-1} \int_{\tau_1+jT_f}^{\tau_1+(j+1)T_f} r(t)v(t-\tau_1-jT_f-c_j{}^{(1)}T_c)dt \tag{3.21}$$

is the test statistic.

The block diagram of the UWB-IR receiver is illustrated in Figure 3.8. It is not easy to detect a single UWB pulse because the monopulse is hidden in the noise of other signals. Therefore, the monopulse looks like noise to other receivers. In order to detect the noise-like transmitted signal, it is necessary to add numerous correlator samples together, which is called pulse integration. With pulse integration, transmitted UWB signals can be demodulated below the noise level. In Figure 3.8, the pulse correlator output, $\alpha_j$, is the output of the pulse correlator, while test statistic, $\alpha$, is the output of the pulse train integrator.

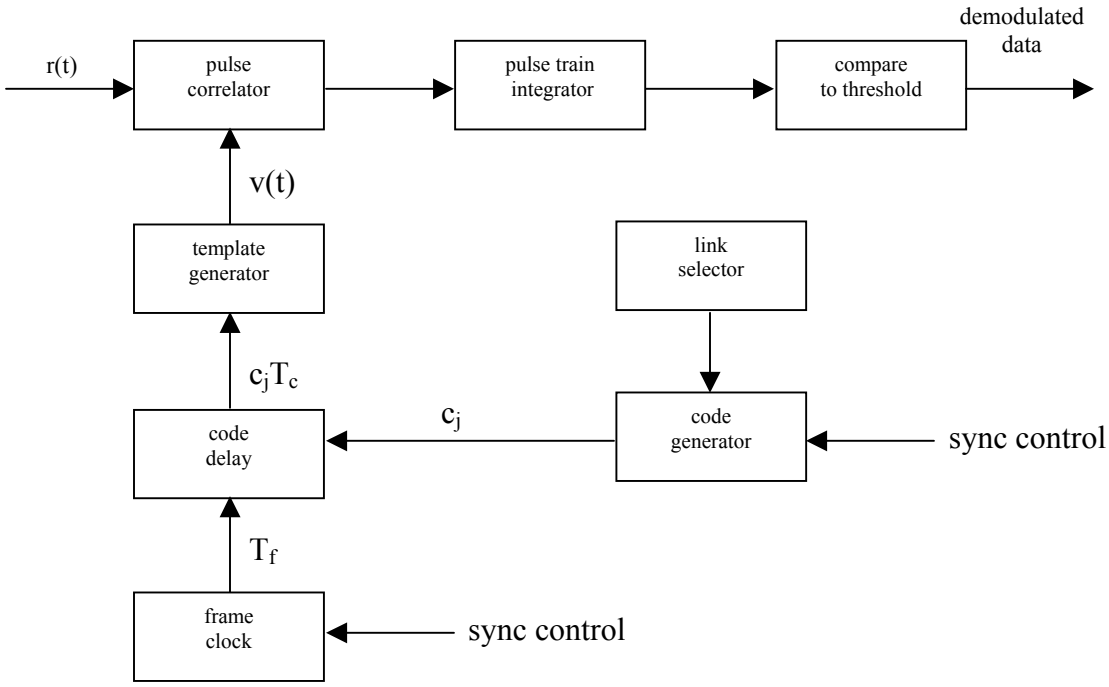


Figure 3.8: Block diagram of the UWB-IR receiver.

# CHAPTER 4
# BER AND PSD COMPARISONS

## 4.1 Pulse Shapes for UWB

The choice of the pulse shape for a UWB system is very important since UWB is a baseband technology and its spectrum is determined by the pulse shape and the pulse duration. There are two goals in selecting the pulse shape for UWB systems [25]. The first goal is to spread the energy in frequency as widely as possible to minimize the PSD and the potential for interference to other systems. The second goal is to avoid a dc component because the ability of the antenna to radiate efficiently decreases as the frequency approaches zero. Various pulse shapes have been proposed for UWB-IR including Gaussian pulse and its derivatives, Manchester, RZ Manchester, sinusoid, and rectangular. In this study, three of the pulse shape candidates are examined: Gaussian first derivative, Gaussian second derivative, and RZ Manchester. These three monopulses are chosen to be investigated in this study because they have been shown to have wider 3-dB bandwidths and no dc component as mentioned in [29]. In addition, these three pulses have balanced positive and negative excursions. Although the first and second order derivatives of Gaussian pulse are examined, Gaussian pulse itself is not included in this study, because it has a dc component. The duration of each pulse is set equal for a fair comparison of modulation schemes.

The most popular pulse shape so far in the literature is the Gaussian first derivative, shown in Figure 3.1. Gaussian first derivative is referred as Gaussian monocycle. In time domain, the Gaussian first derivative is mathematically equivalent to the first derivative of the Gaussian function, which has the form:

$$w(t) = A\pi f_c t e^{-2(\pi f_c (t-t_c))^2} . \tag{4.1}$$

Here, A is the amplitude, and $f_c$ is the center frequency, which is the reciprocal of the monopulse duration, and $t_c$ is the time shift.

Another pulse shape candidate for UWB is the Gaussian second derivative, which is also referred as Gaussian doublet, Scholtz monocycle or Rayleigh monocycle. Figure 4.1 shows the Gaussian second derivative in time domain. In time domain, the monopulse can be expressed as:

$$w(t) = A(1 - 4\pi(f_c(t - t_c))^2)e^{-2\pi(f_c(t-t_c))^2}. \quad (4.2)$$

The last monopulse to be examined is RZ-Manchester. Figure 4.2 shows the RZ-Manchester monopulse in time domain. The monopulse can be mathematically defined as

$$w(t) = -\sqrt{\frac{A}{\tau}}, \qquad (t_c+\tau/6<t< t_c+\tau/2)$$

$$w(t) = +\sqrt{\frac{A}{\tau}}, \qquad (t_c-\tau/2<t< t_c-\tau/6) \quad (4.3)$$

$$w(t) = 0. \qquad (t_c-\tau/6<t< t_c+\tau/6)$$

Following is the definition of the three modulation schemes to be compared using the above pulse shapes.

## 4.2 Modulation Schemes for UWB

The selection of the modulation scheme for a UWB-IR system is important because it affects the BER performance as well as the PSD of the system. PPM, OOK, and BPSK are the modulation schemes to be compared via Matlab simulation. PPM uses an orthogonal signaling scheme and has been the most popular modulation scheme used in literature for UWB communication systems so far. On the other hand, OOK has an advantage of easy implementation [4]. Another candidate for modulation of UWB-IR, BPSK, uses an antipodal signaling scheme and has been gaining acceptance recently due

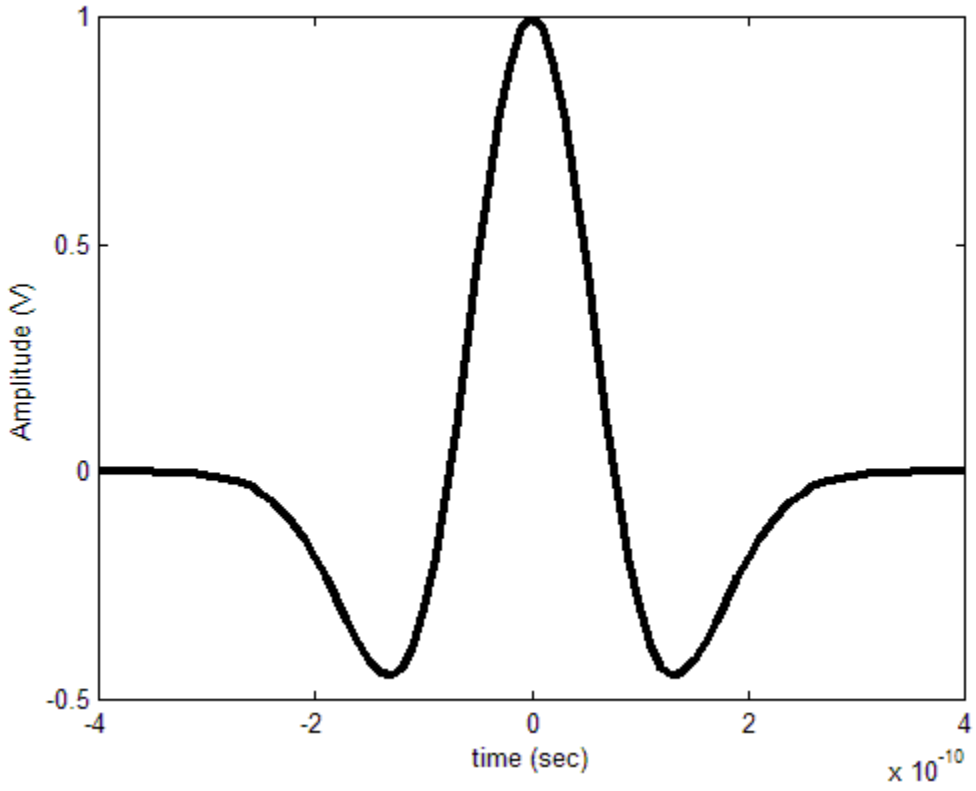


Figure 4.1: Gaussian second derivative pulse in time domain.

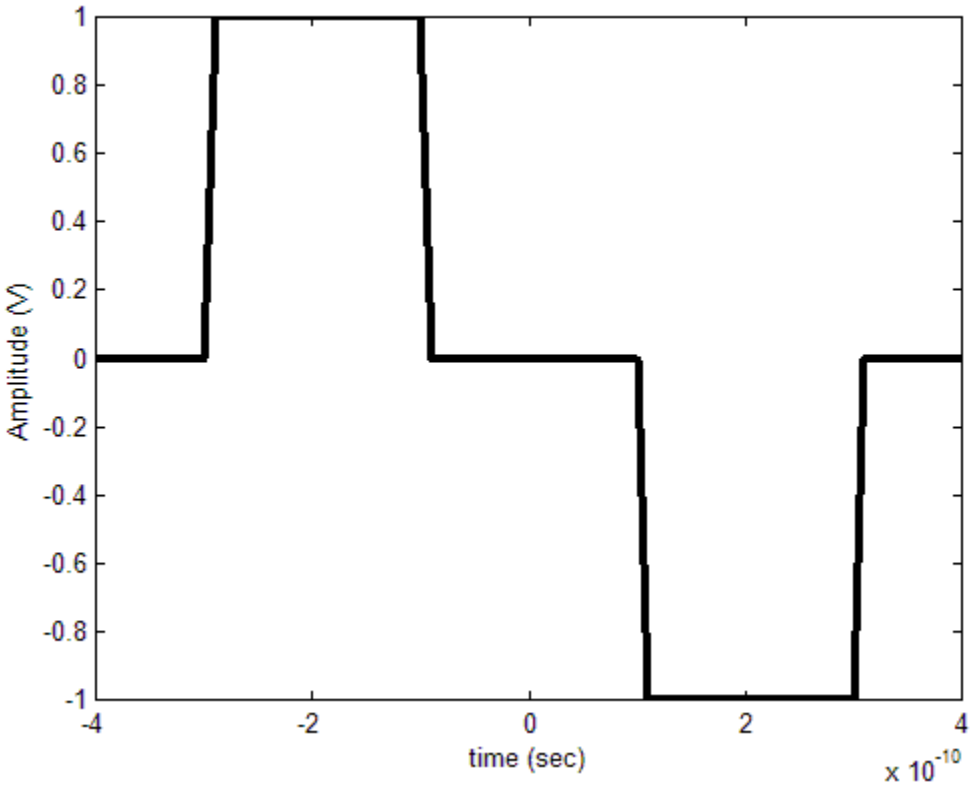


Figure 4.2: RZ-Manchester pulse in time domain.

to its high energy efficiency. A UWB pulse train signal is represented as a sum of pulses shifted in time in [32] as:

$$s(t) = \sum_j a_j w(t - t_j), \tag{4.4}$$

where, s(t) is the modulated UWB signal, w(t) is the transmitted UWB pulse shape, $a_j$ is the amplitude offset and $t_j$ is the time offset. A general equation for every modulation scheme is expressed as:

$$s(t) = \sum_j a_j w(t - jT_f - c_j T_c - \delta d_j), \tag{4.5}$$

where, $t_j = jT_f + c_j T_c + \delta d_j$, $T_f$ is the pulse repetition time or frame time, $c_j$ is the time hopping code sequence with an additional time shift of $c_j T_c$ to the $j^{th}$ pulse, $\delta$ is the modulation factor, and d is the binary (0 or 1) bit stream data sequence. The parameters in (4.5) for three modulation schemes are given in Table 4.1. Following is a review of each modulation scheme.

### 4.2.1 PPM

PPM modulation format can be written as

$$s(t) = \sum_j a_j w(t - jT_f - c_j T_c - \delta_{opt} d_j). \tag{4.6}$$

Table 4.1: UWB modulation scheme parameters.

| **Modulation Scheme** | $\mathbf{a_j}$ | $\mathbf{\delta d_j}$ |
|---|---|---|
| PPM | 1 | 0, $\delta_{opt}$ |
| OOK | 0, 1 | 0 |
| BPSK | ±1 | 0 |

In this modulation method, if the data bit is 0, no additional time shift is modulated on the monopulse, but a time shift of δ is added to a monopulse if the bit is 1. Figure 4.3 shows PPM data using Gaussian first derivative. The parameter $\delta_{opt}$ in (4.6) is a modulation factor, which is expressed in [3] as:

$$\delta_{opt} = \arg\min_{\delta} \int_{-\infty}^{\infty} w(t)w(t-\delta)dt \,. \tag{4.7}$$

The choice of the modulation parameter determines the performance. The value of the parameter is different for every pulse shape.

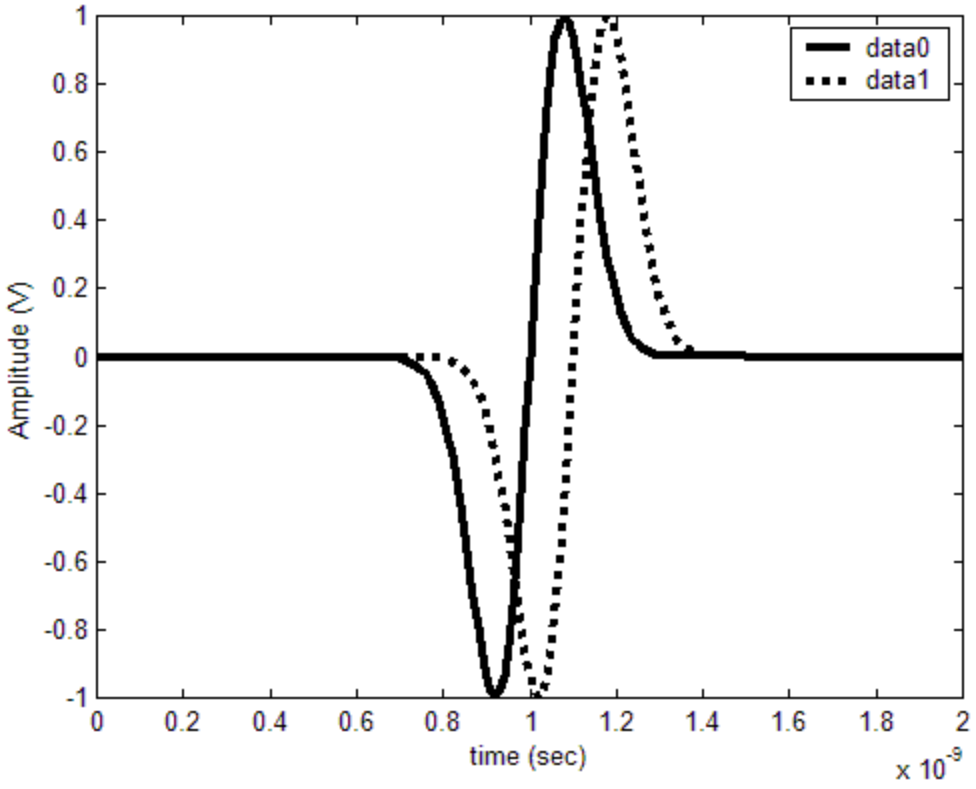


Figure 4.3: PPM data using Gaussian first derivative pulse.

### 4.2.2 OOK

OOK data modulation format is

$$s(t) = \sum_j a_j w(t - jT_f). \tag{4.8}$$

In this modulation method, the presence of a pulse indicates the data bit 1 while no pulse indicates the data bit 0. Figure 4.4 shows OOK data using Gaussian first derivative.

### 4.2.3 BPSK

BPSK data modulation format is given by

$$s(t) = \sum_j \pm a_j w(t - jT_f). \tag{4.9}$$

In this modulation method, the data is carried in the polarity of the pulse. The phase value of zero degrees indicates the data bit 1 while the phase value of 180 degrees indicates the data bit 0. Figure 4.5 shows BPSK data using Gaussian first derivative.

## 4.3 BER Comparisons

For narrowband systems, the bit error probability or BER depends on the received SNR. The BER may be expressed in terms of the distance between the two signals. Figure 4.6 shows the constellation diagrams of PPM, OOK, and BPSK modulation schemes, respectively. The performance of PPM, which uses orthogonal signaling scheme, is identical to the performance of OOK. This is not surprising because OOK is a special case of orthogonal signaling [35]. If the BER is compared with the BER for binary PPM and OOK, it is found that binary PPM and OOK require an increase of factor of 2 in energy to achieve the same BER as BPSK signals. Since $10\log_{10}2 = 3$, binary PPM and OOK signals are 3 dB poorer than BPSK signals in BER comparisons. The difference of 3 dB is simply due to the distance between the two signal points. In conclusion, for equal energy per bit, BPSK has greater inter-symbol distance than binary

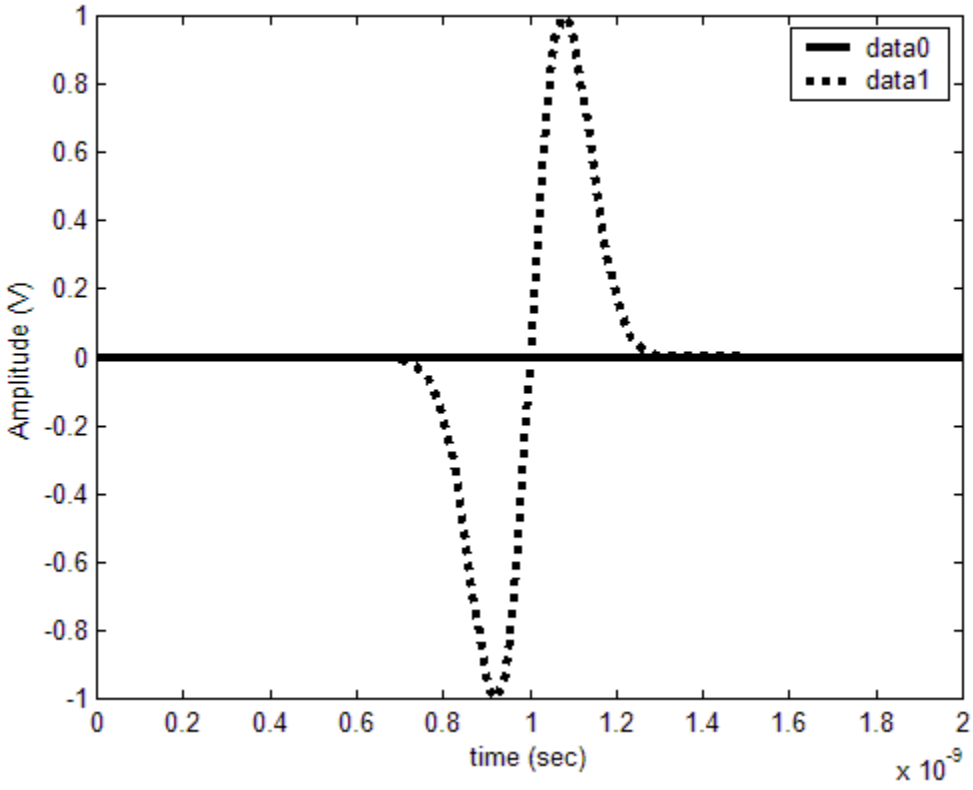


Figure 4.4: Gaussian first derivative pulse with OOK data.

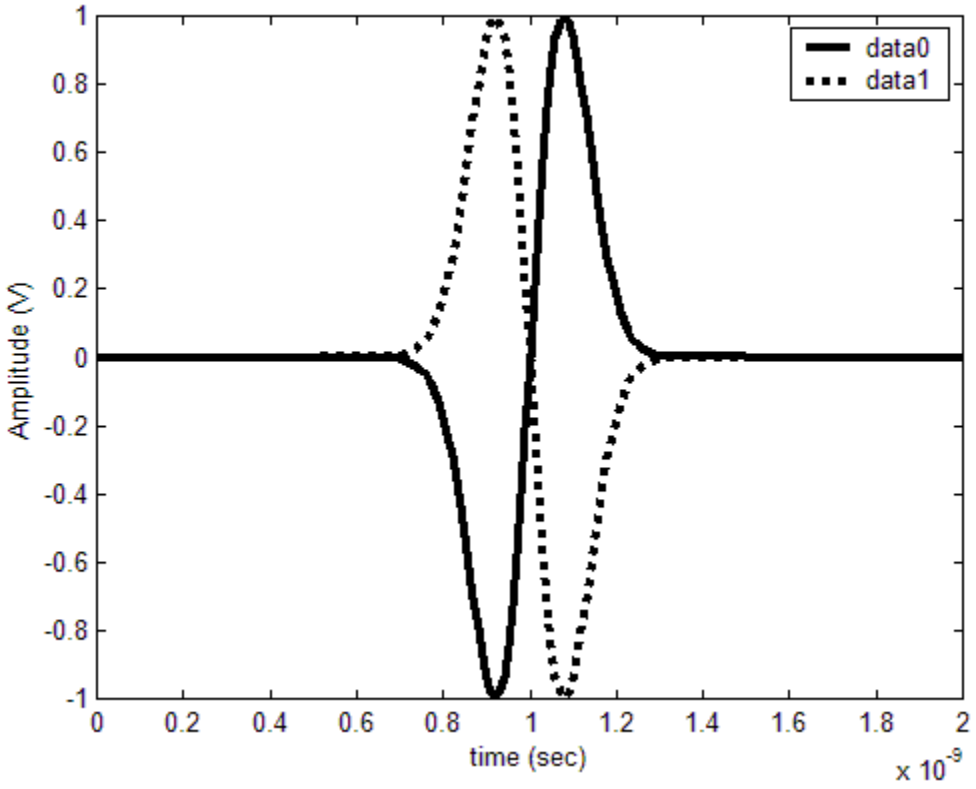


Figure 4.5: BPSK data with Gaussian first derivative pulse.

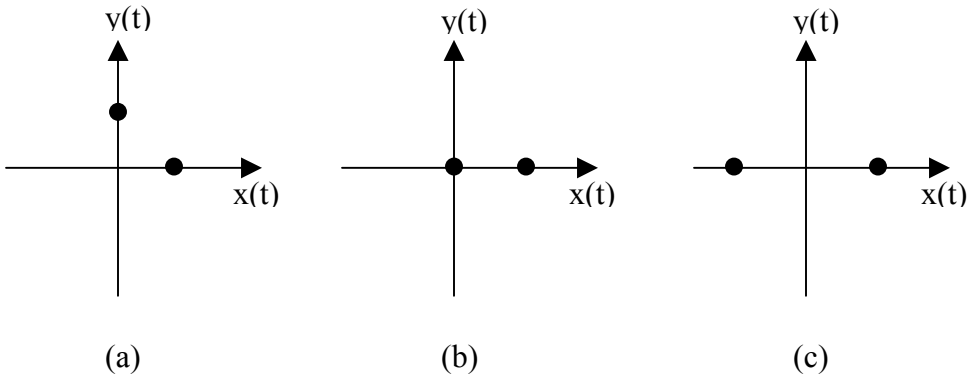


Figure 4.6: Constellation diagrams of (a) PPM (b) OOK (c) BPSK modulation schemes.

PPM and OOK. This means that binary PPM requires more energy than BPSK to achieve the same BER. Thus, BPSK has an advantage over binary PPM and OOK in energy efficiency.

Three possible pulse shapes and three possible binary modulation schemes are analyzed to investigate their effects on the performance of UWB-IR. Each pulse duration is set to 0.6 ns for a fair comparison and no time-hopping code is used, i.e. $c_j = 0$. The BER performances of the system for these three pulse shapes and three modulation schemes are compared for both AWGN channel and Rayleigh fading channel, respectively, using a correlation receiver.

Figure 4.7 shows the BER performance comparison in AWGN channel. The notations 'gaus1st', 'gaus2nd', and 'rz-manc' represent Gaussian first derivative, Gaussian second derivative, and RZ Manchester, respectively. The plots in Figure 4.7 present that BPSK presents the best performance for all pulse shapes while PPM offers advantage over OOK for Gaussian first and second derivatives. The result of this comparison for UWB-IR systems is similar to the bit error rate comparison of the same three modulation schemes for narrowband systems.

Figure 4.7 shows that in PPM, the Gaussian second derivative performs the best while Gaussian first derivative performs better than the RZ-Manchester pulse for all SNR values. On the other hand, it is very clear from the plots that different pulse shapes do not significantly affect the performance for OOK and BPSK modulation schemes. Overall, RZ-Manchester using BPSK modulation scheme is observed to give the best performance in AWGN channel only.

Figure 4.8 presents the BER performance comparison in Rayleigh fading channel. The plots in Figure 4.8 show that BPSK gives the best performance, as in AWGN channel only, and PPM offers advantage over OOK for all pulse shapes. Like the performance for PPM in AWGN channel only, the Gaussian second derivative performs the best while Gaussian first derivative performs better than the RZ-Manchester pulse for all SNR values. In OOK, all pulse shapes give similar performance for low SNR values while RZ-Manchester gives better performance than Gaussian first and second derivatives for higher SNR values. For BPSK, all pulse shapes give similar performance

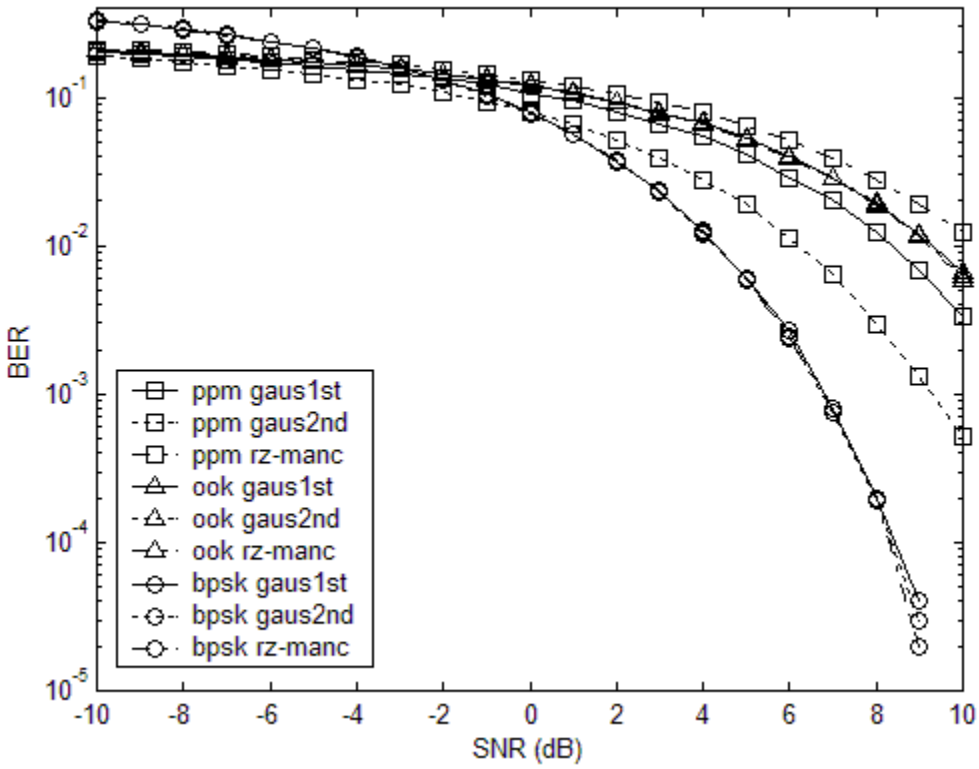


Figure 4.7: BER performances in AWGN channel for three modulation schemes and three pulse shapes.

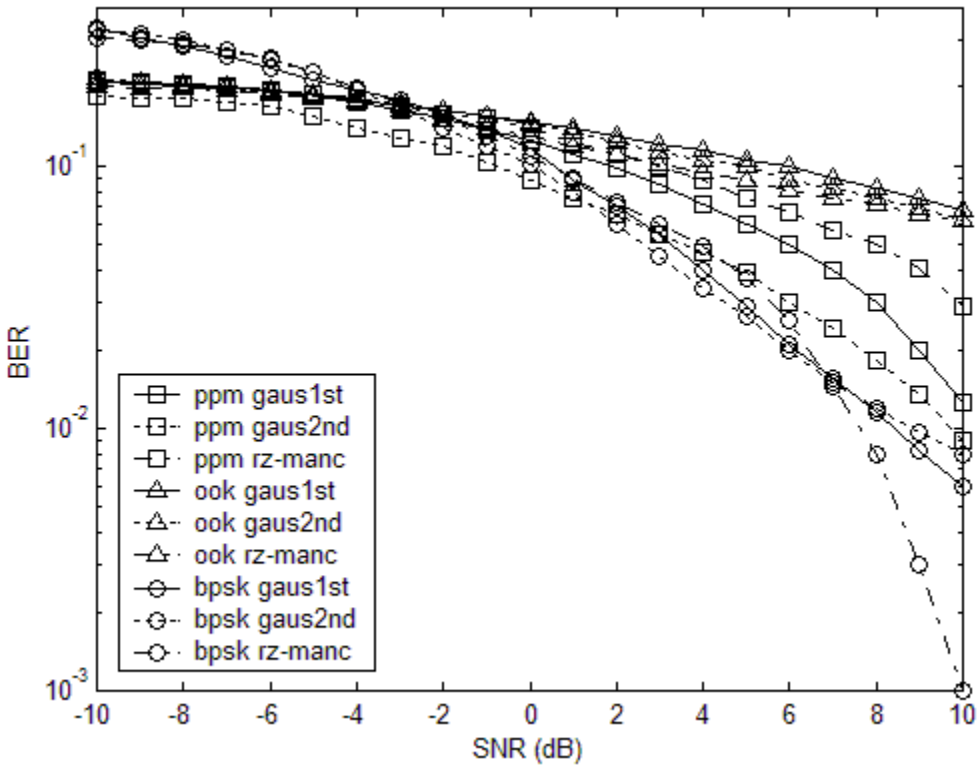


Figure 4.8: BER performances in Rayleigh fading channel.

but RZ-Manchester offer advantage to Gaussian first and second derivatives for very high SNR values. Overall, RZ-Manchester using BPSK modulation scheme seems to give the best performance in Rayleigh fading channel.

## 4.4 PSD Comparisons

The PSD is defined as the average power in the signal per unit bandwidth. PSD provides information on how the power is distributed over RF spectrum. It is another interest of this thesis to understand the spectral characteristics of UWB-IR signals via computer simulations by observing the changes in their temporal characteristics. The shape of the PSD for a UWB-IR system is very important because PSD determines the

relation between the UWB-IR system and other existing systems in the spectrum. Figure 4.9 shows the PSD of Gaussian first derivative pulse with pulse duration of 0.5ns.

In the time domain, UWB-IR pulse train looks regular since the pulses are equally apart from each other. Figure 4.10 shows the PSD of UWB-IR pulse train with 10 monopulses in a bit, Ns=10. The pulse train produces energy spikes in the frequency domain, which look like comb lines as seen in Figure 4.11. The low UWB signal power is spread among these comb lines. On the contrary, the spectrum of a signal needs to be smooth in order to be less detectable. In other words, smoothness of a signal makes the signal less likely to interfere with the narrowband and wideband signals that share the same spectrum. Therefore, the fewer comb lines a signal has, the smoother that signal becomes in the spectrum. The pulse-to-pulse intervals need to be varied to eliminate the comb lines. This can be achieved by using modulation and pseudorandom codes.

Pulse duration, pulse repetition rate, modulation scheme, and use of pseudorandom codes are the determinants on the performance of the PSD for a UWB-IR system. In this chapter, the effects of the above parameters are investigated on the PSD of a UWB-IR system.

### 4.4.1 Effect of Pulse Duration

The pulse duration is one of the determinants on the PSD of a UWB-IR pulse. Figure 4.12 shows that when the pulse duration is halved, T=0.25 ns, the spectrum gets wider while the amplitude gets halved as well.

### 4.4.2 Effect of Pulse Repetition Rate

Another factor affecting the PSD of a UWB-IR signal is the pulse repetition rate. Changing the pulse rate in a UWB-IR system affects the magnitude of the PSD as well. When the pulse rate is halved, Ns=5, it can be clearly seen in Figure 4.13 that the amplitude of the PSD gets halved as well.

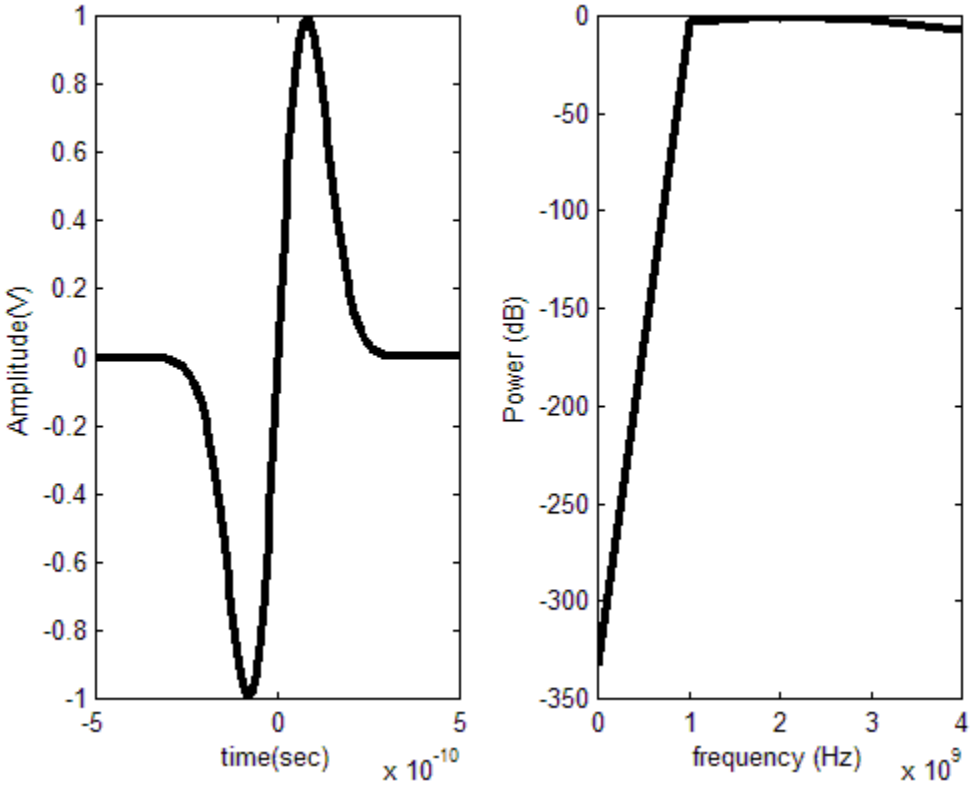


Figure 4.9: PSD of Gaussian first derivative pulse with duration of 0.5ns.

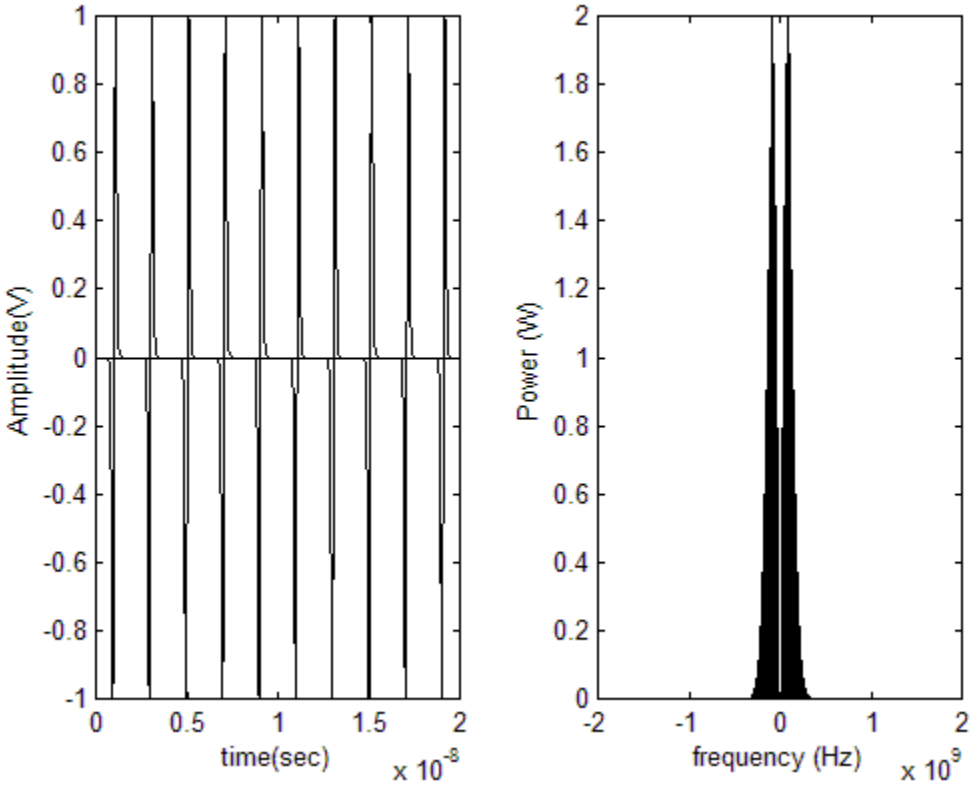


Figure 4.10: PSD of pulse train ($N_s$=10).

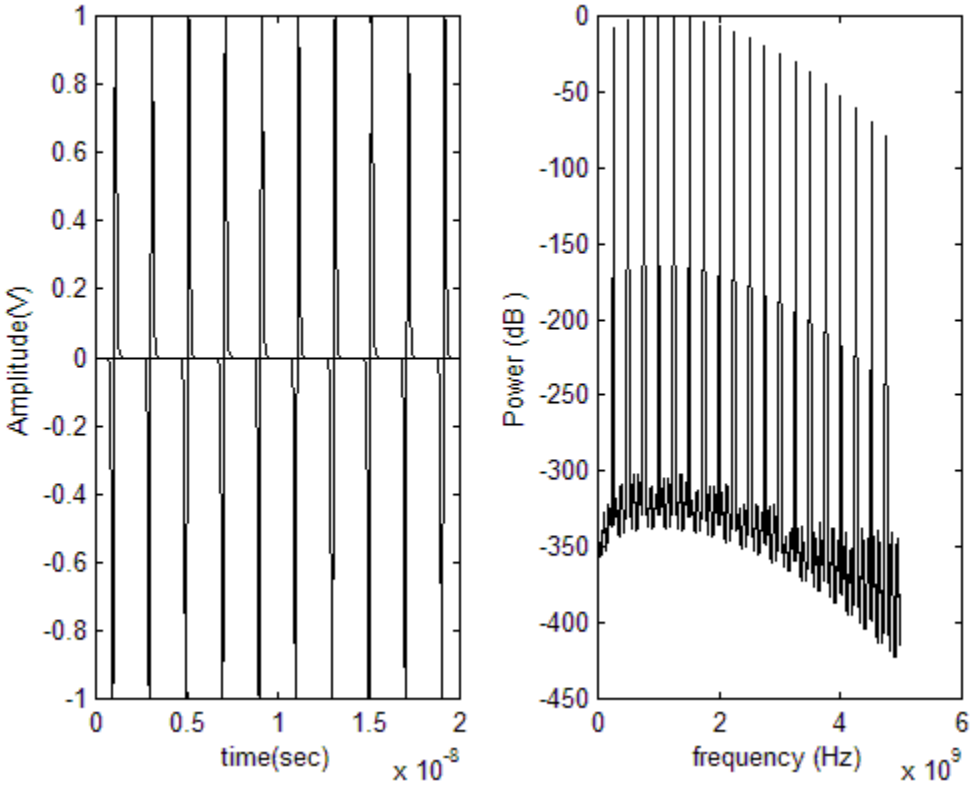


Figure 4.11: PSD of Gaussian first derivative pulse in dB (Ns=10).

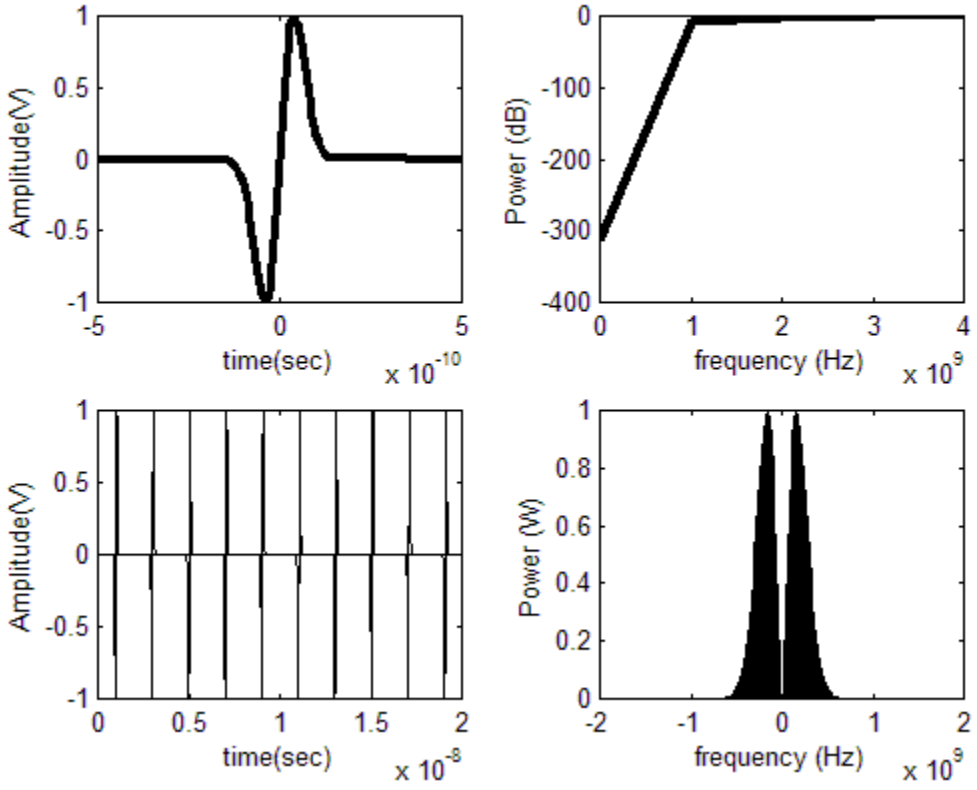


Figure 4.12: PSD of pulse train of halved pulse duration of 0.25 ns.

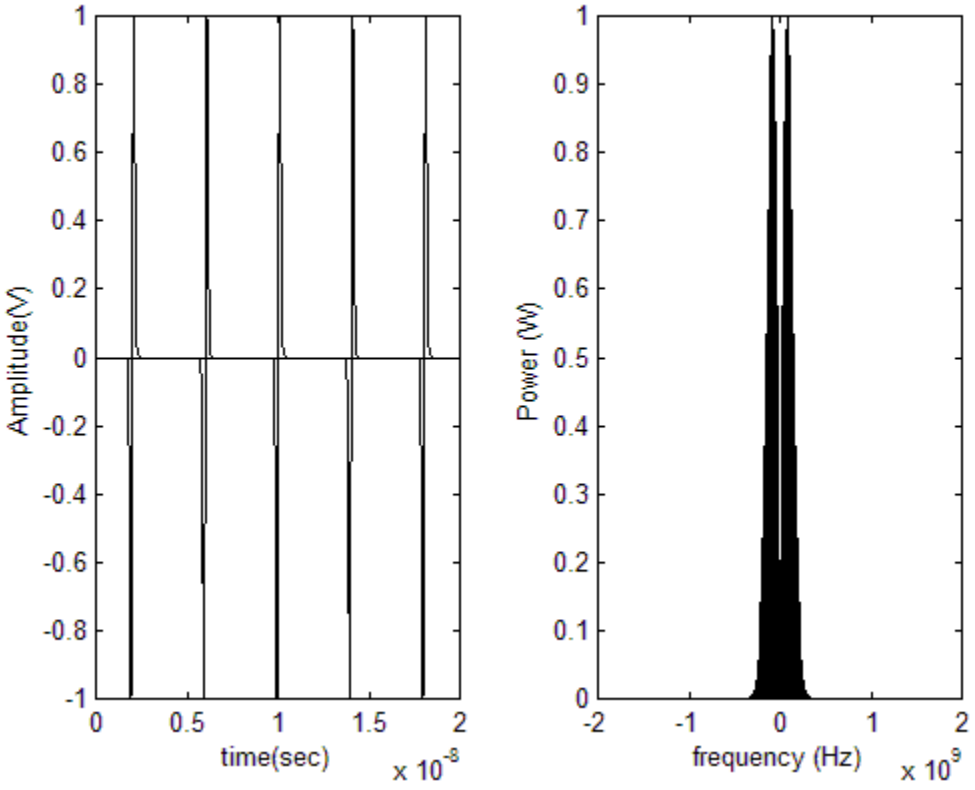


Figure 4.13: PSD of pulse train with halved pulse rate (Ns=5).

### 4.4.3 Effect of Modulation Scheme

A UWB-IR pulse train signal is the sum of pulses shifted in time and is expressed as:

$$s(t) = \sum_j a_j w(t - t_j) . \tag{4.10}$$

Assuming the pulses are uniformly spaced in time, i.e. $t_j = jT_f$, (4.10) becomes:

$$s(t) = \sum_j a_j w(t - jT_f) . \tag{4.11}$$

The PSD is the Fourier transform of the autocorrelation of the signal. It is assumed that the pulse weights correspond to the data bits to be transmitted. The data are assumed to be random [30]. The PSD of (4.11) can be found by the method in [34]:

$$\Phi_{ss}(f) = \frac{\sigma_a^{\,2}}{T_f}\left|W(f)\right|^2 + \frac{\mu_a^{\,2}}{T_f^{\,2}}\sum_{k=-\infty}^{\infty}\left|W(\frac{j}{T_f})\right|^2 \delta(f - \frac{j}{T_f}) , \tag{4.12}$$

where, $\sigma_a^2$ and $\mu_a$ are the variance and mean of the weight sequence, respectively, W(f) is the Fourier transform of w(t), and $\delta$(f) is a unit impulse. The expression in (4.12) can be separated into two terms to visualize the two different types of spectral components. The first term is the continuous spectrum, in which its shape depends only on the spectral characteristics of the shaping pulse, w(t). The second term is the discrete spectrum and is composed of discrete spectral lines. As seen in (4.12), the magnitude of the discrete spectral lines depends on the mean of the weight sequence. This shows that the modulation scheme plays an important role in PSD of the signal. It is not desirable for UWB-IR communications systems to include discrete frequency components because of possible interference with the existing systems. The discrete frequency components disappears only if the data bits have zero mean, i.e. $\mu_a^2$=0.

When OOK is used, $a_j \in [0,1]$. The mean or expected value of the sequence becomes, $E(a) = \mu_a = (0+1)/2$, or 0.5. The variance of the sequence becomes, $\sigma_a^2 = E(a^2) - (E(a))^2 = (0^2+1^2)/2 - (0.5)^2 = 0.25$. The data bits are assumed to be random and have equal probability. The PSD for OOK is found by the method in [30] as:

$$\Phi_{ss-OOK}(f) = \frac{1}{4T_f}|W(f)|^2 + \frac{1}{4T_f^{\,2}}\sum_{k=-\infty}^{\infty}\left|W(\frac{j}{T_f})\right|^2 \delta(f-\frac{j}{T_f}). \quad (4.13)$$

Figure 4.14 shows the simulation result for PSD of pulse train and PSD of OOK with data [0 1]. It can clearly be seen that PSD of OOK consists of spectral lines.

When BPSK is used, $a_j \in [-1,1]$. The mean or expected value of the sequence becomes, $E(a) = \mu_a = (-1+1)/2$, or 0. The variance of the sequence becomes $\sigma_a^2 = E(a^2) - (E(a))^2 = (-1^2+1^2)/2 - (0)^2 = 1$. Again, the data bits are assumed to be random and have equal probability. The PSD for BPSK is found by the method in [30] as

$$\Phi_{ss-BPSK}(f) = \frac{1}{T_f}|W(f)|^2. \quad (4.14)$$

Since BPSK has a mean of zero, the discrete frequency components become zero as seen in (4.14), thus no spectral lines exist in the PSD of a BPSK system as seen in Figure 4.15.

When PPM is used, the pulses are not uniformly spaced as they are in OOK and BPSK. From Table 4.1, $a_j=1$ and $d_j \in [0,\delta_{opt}]$. The derivation of the PSD for PPM scheme is more complex than the ones for OOK and BPSK. Although a general form of PSD for PPM is not present, PPM does include spectral lines on its PSD as shown in Figure 4.16.

### 4.4.4 Effect of Pseudorandom Codes

Time hopping introduces randomness into the transmitted signal in order to enhance the robustness and accommodate multiple users. Pseudorandom coding varies

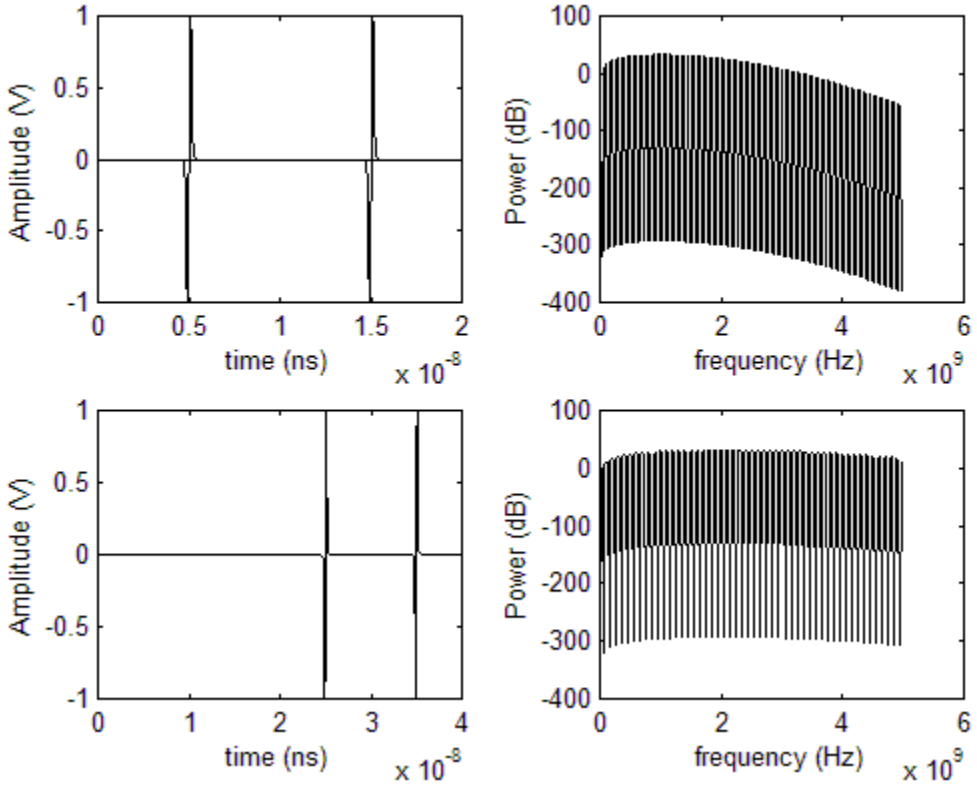


Figure 4.14: PSD of pulse train and OOK with data [0 1].

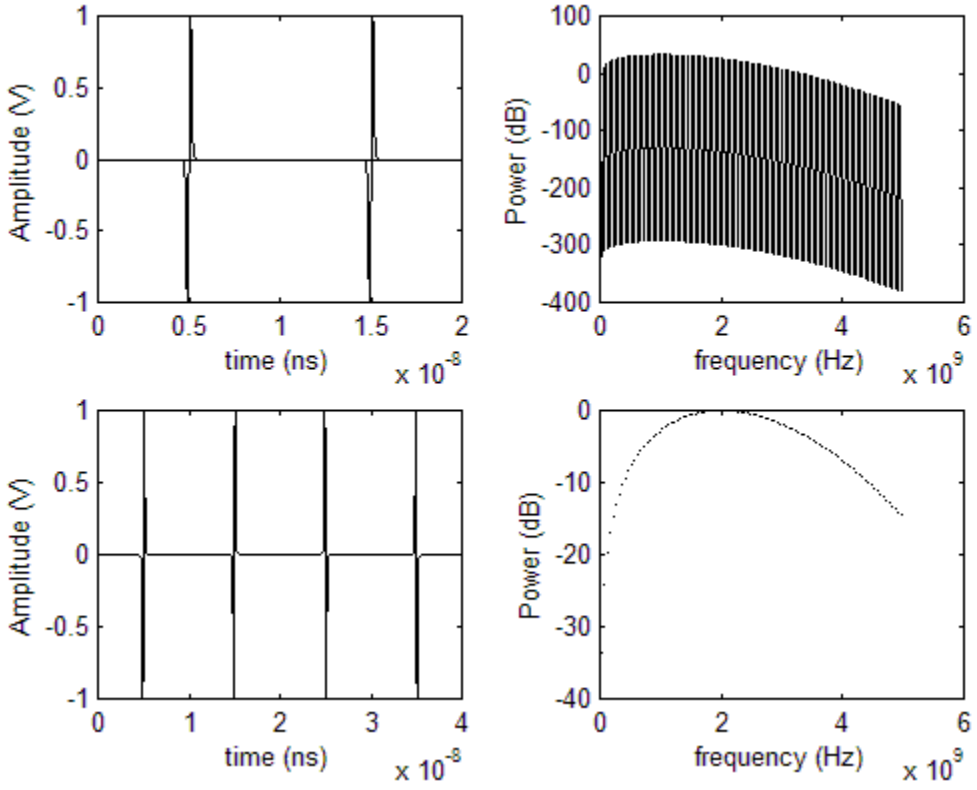


Figure 4.15: PSD of pulse train and BPSK with data [0 1].

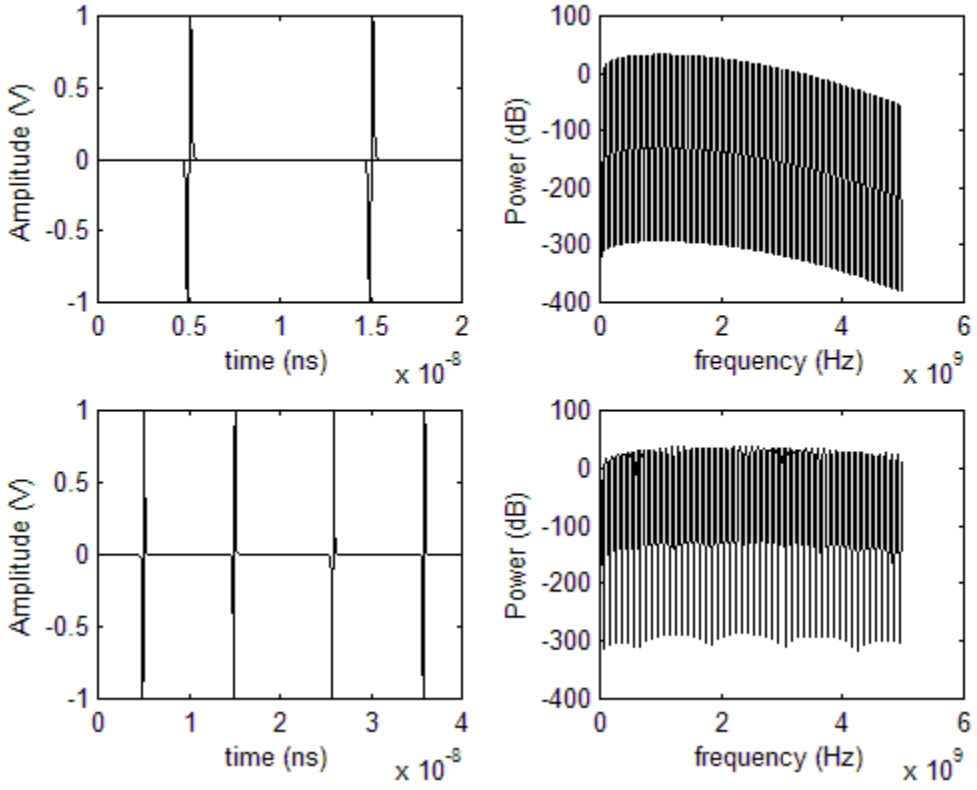


Figure 4.16: PSD of pulse train and PPM with data [0 1].

pulse-to-pulse intervals, which helps to eliminate the discrete lines. As seen in Figure 4.17, PSD of the PPM scheme consists of energy spikes. Pseudorandom code eliminates these energy spikes by shifting each monopulse. Therefore, the frequency spectrum is spread randomly and produces less power in magnitude in discrete lines.

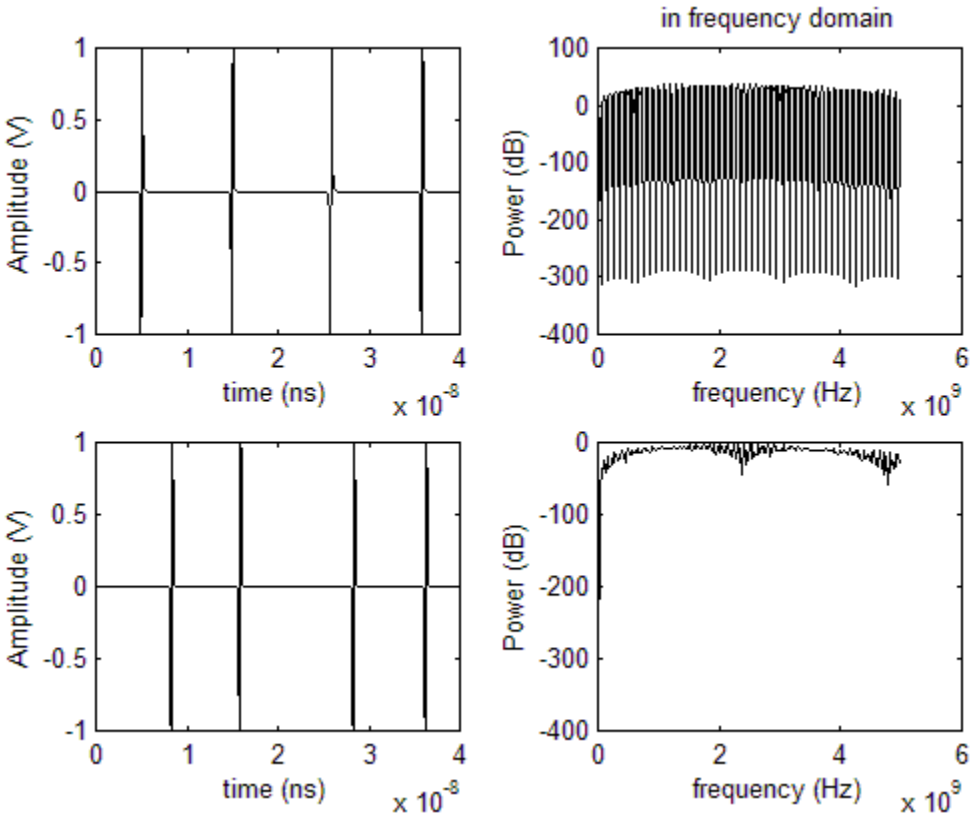


Figure 4.17: PSD of PPM with data [0 1] and code.

# CHAPTER 5
# CONCLUSION

UWB-IR is a wireless communications technology whose development is in progress and has been a hot topic in the literature. The technology transmits and receives millions of ultra short signals in the already allocated RF spectrum by hiding the transmission below the noise level. The technology is characterized by wide bandwidth, high spatial capacity, and very low power transmission. These features make UWB-IR a strong candidate for local and personal area networks, radar, imaging, and position location estimation applications. UWB-IR has received considerable attention after its regulation on February 14, 2002. Many companies already adopted this new powerful technology because of its promising features and its advantages over the existing systems. On the other hand, many others feel concerned with its existence because of its possible interference with their systems on licensed bands and its free use.

Many research have been done on the different aspects of UWB-IR technology. In this thesis, the temporal and spectral characteristics of UWB-IR are studied. First, three possible pulse shapes and three possible modulation schemes are investigated for UWB-IR. Followed by, their BER performance in AWGN channel only and in Rayleigh fading channel are simulated and compared. Finally, the effects of essential UWB-IR parameters on the PSD are investigated via simulations.

The simulation results show that the shape of the waveform affects the BER performances of PPM scheme in both channels while it has a small effect on the performance of OOK and BPSK modulation schemes. The BER performance of BPSK modulation scheme using RZ-Manchester pulse is observed to be the best in both channels. BPSK offer advantage over PPM and OOK in the PSD analysis as well. Because it has zero mean, the PSD of BPSK includes no discrete spectrum. PPM and OOK modulation schemes have the disadvantage of creating high discrete spectral lines.

The effects of other parameters on the PSD are also investigated in this study. The pulse duration is found to have an effect on both the amplitude and the width of the PSD.

The PSD amplitude is decreased with a decrease in pulse duration. The second parameter, pulse repetition rate, is found to have an effect on the amplitude of the PSD as well. This is because, when the pulse rate is decreased, the average power decreases. Less average power yields to smaller duty cycles. Thus, the amplitude of PSD gets smaller. The last parameter, pseudorandom codes, is proved to have positive effect on minimizing the discrete spectral lines of PSD because the pseudorandom codes introduce randomness to the signal and varies the pulse-to-pulse interval. In summary, the use of pseudorandom codes not only provides privacy to each user, but also helps the system to share its spectrum with the existing users without interference. Even though PPM gives better performance than OOK in BER comparison, it has high discrete lines on its PSD. In conclusion, BPSK modulation scheme is power efficient and has an advantage with the absence of any discrete lines on its PSD.

Three pulse shapes were presented in this study. In the future studies more different pulse shapes for UWB-IR, whose characteristics meet the requirements, may be investigated and their BER performances may be compared. The performance of the UWB-IR is studied in this thesis for a single user only. Because the performance of the modulation schemes for a single user may not present the same performance for multiple users, the performance of different modulation schemes using pseudorandom codes may be investigated for multiple users as well.

UWB has received enormous attention from companies and universities all around the world. The future of UWB technology in the United States will depend on its development in research as well as FCC's decisions on regulations on its usage.

# REFERENCES

[1] J. Foerster, E. Green, S. Somayazulu, and D. Leeper, "Ultra-wideband technology for short- or medium-range wireless communications," *Intel Technology Journal,* Q2, 2001.

[2] P. Withington, "Impulse radio overview," Time Domain Corporation, www.timedomain.com, July 2001.

[3] R. Scholtz, "Multiple access with time-hopping impulse modulation," *Proc. MILCOM*, vol. 2, pp. 447-450, Oct. 1993.

[4] R. Fontana, "On range-bandwidth per joule for ultra-wideband and spread spectrum waveforms," Multispectral Solutions Inc., www.multispectral.com, July 2000.

[5] R. Fontana, "A brief history of UWB communications," Multispectral Solutions Inc., www.multispectral.com.

[6] OSD/DARPA, Ultra-Wideband Radar Review Panel, Assessment of Ultra Wideband (UWB) Technology, DARPA, Arlington, VA, 1990.

[7] M. Z. Win and R. A. Scholtz, "Comparisons of analog and digital impulse radio for wireless multiple-access communications," *Proc. IEEE Int. Conf. on Comm.*, pp. 91-95, June 1997, Montreal, Canada.

[8] M. Z. Win and R. A. Scholtz, "Impulse radio: How it works," *IEEE Communications Letters*, vol. 2, no. 2, pp 36-38, Feb. 1998.

[9] M. Z. Win and R. A. Scholtz, "Ultra-wide bandwidth time-hopping spread-spectrum impulse radio for wireless multiple-access communications," *IEEE Transactions on Communications*, vol. 48, no. 4, 679-689, Apr 2000.

[10] F. Ramirez-Mireles and Robert A. Scholtz, "Multiple-access with time hopping and block waveform PPM modulation," *Proc. Int. Conf. Comm.*, vol. 2, pp. 775-779, 1998, Toronto, ON, Canada.

[11] F. Ramirez-Mireles, "Performance of ultrawideband SSMA using time hopping and M-ary PPM". *IEEE Journal on Selected Areas in Communications*, vol. 19, no. 6, pp. 1186-1196, June 2001.

[12] R. J. - M. Cramer, Moe. Z. Win, and Robert A. Scholtz, "Evaluation of the multi-path characteristics of the imp*ulse radio channel," Proc. IEEE 9th Int. Symp.*

*Indoor Mobile Radio Communications,* vol. 2, pp. 864-868, Sep. 1998.

[13] R. J. – M. Cramer, Moe. Z. Win, and Robert A. Scholtz, "Impulse radio multi-path characteristics and diversity reception," *Proc. ICC*, pp. 1650-1654, June 1998.

[14] R. J. - M. Cramer, Moe. Z. Win, and Robert A. Scholtz, "Evaluation of the propagation characteristics of ultra-wideband communication channels," *Proc. PIMRC '98*, vol. 2, pp. 626-630, Sep. 1998, Boston, USA.

[15] R. J.-M. Cramer, M. Z. Win, and R. A. Scholtz, "On the analysis of UWB communication channels," *Proc. MILCOM*, pp. 1191-1195, Nov. 1999.

[16] F. Ramirez-Mireles, "On the performance of ultra-wide-band signals in Gaussian noise and dense multipath," *IEEE Transactions on Vehicular Technology*, vol. 50, pp. 244-249, Jan. 2001.

[17] F. Ramirez-Mireles, M. Z. Win, and R. A. Scholtz, "Performance of Ultra-Wideband Time-Shift-Modulated Signals in the Indoor Wireless Impulse Radio Channel," The 31st Asilomar Conference on Signals, Systems & Computers, vol. 1, pp. 192-196, Nov. 1997.

[18] H. Lee, B. Han, Y. Shin, and S. Im, "Multipath characteristics of impulse radio channels," IEEE 51st Vehicular Technology Conference, vol. 3, pp. 2487-2491, Spring 2000.

[19] M. Ho, V. S. Somayazulu, J. Foerster, and S. Roy, "A differential detector for an ultra-wideband communications system," IEEE 55th Vehicular Technology Conference, vol. 4, pp. 1896-1900, May 2002.

[20] F. Ramirez-Mireles and R. A. Scholtz, "Performance of equicorrelated ultra-wideband pulse-position-modulated signals in the indoor wireless impulse radio channel," IEEE Pacific Rim Conference on Communications, Computers and Signal Processing, vol. 2, pp. 640-644, Aug. 1997.

[21] F. Ramirez-Mireles, M. Z. Win, and R. A. Scholtz, "Signal selection for the indoor wireless impulse radio channel," IEEE 47th Vehicular Technology Conference, vol. 3, pp. 2243-2247, May 1997.

[22] M. Z. Win and Robert A. Scholtz, "On the energy capture of ultrawide bandwidth signals in dense multi-path environments," *IEEE Comm. Lett.*, vol. 2, pp. 245-247,

Sep. 1998.

[23] M. Z. Win and Robert A. Scholtz, "On the robustness of ultra-wide bandwidth signals in dense multi-path environments," *IEEE Comm. Lett.*, vol. 2, pp. 51-53, Feb. 1998.

[24] R. J.-M. Cramer, M. Z. Win, and R. A. Scholtz, "Spatio-temporal diversity in ultra-wideband radio," IEEE Wireless Comm. And Networking Conf., vol. 2, pp. 888-892, Sep. 1999.

[25] L. Zhao and A. Haimovic, "Performance of ultra-wideband communications in the presence of interference," *IEEE Journal on Selected Areas in Communications*, vol. 20, pp. 1684-1692, Dec. 2002.

[26] J. R. Foerster, "Interference modeling of pulse-based UWB waveforms on narrowband systems," IEEE 55th Vehicular Technology Conference, vol. 4, pp. 1931-1935, May 2002.

[27] A. Muqaibel, B. Woerner, and S. Riad, "Application of multi-user detection techniques to impulse radio time hopping multiple access systems," IEEE Conference on Ultra Wideband Systems and Technology, May 2002.

[28] J. D. Choi and W. E. Stark, "Performance of Ultra-Wideband Communications With Suboptimal Receivers in Multipath Channels," *IEEE Journal on Selected Areas in Communications,* vol. 20, no. 9, Dec. 2002

[29] X. Chen and S. Kiaei, "Monocycle shapes for ultra wideband system," IEEE International Symposium on Circuits and Systems, vol. 1, pp. 597 –600, May 2002.

[30] M. L. Welborn, "System considerations for ultra-wideband wireless networks," IEEE Radio and Wireless Conference, pp. 5-8, Aug. 2001.

[31] H. Sheng, P. Orlik, A. M. Haimovic, L. J. Cimini Jr., and J. Zhang, "On the spectral and power requirements for ultra-wideband transmission," IEEE Int. Conf. On Comm. ICC, vol. 1, pp. 738-742, May 2003.

[32] M. Welborn and J. McCorkle, "The importance of fractional bandwidth in ultra-wideband pulse design," IEEE International Conference on Communications, vol. 2, pp. 753-757, Oct. 2002.

[33] X. Huang and Y. Li, "Generating near-white ultra-wideband signals with period extended PN sequences," IEEE VTS 53rd Vehicular Technology Conference, vol. 2, pp. 1184-1188, Spring 2001.

[34] J. G. Proakis, *Digital Communications*, Fourth Edition, McGraw-Hill, Inc., 2001.

[35] B. P. Lathi, *Modern Digital and Analog Communication Systems*, Third Edition, Oxford Unv. Press, Inc. 1996.

# VITA

Ömer Sezer was born in Eskişehir, Turkey on August 19, 1977. He graduated from Private Yakindogu High School in 1995. Then, he entered the Electrical and Electronics Engineering Department of Osmangazi University, Eskisehir. He received a B.S. in electrical and electronics engineering in 1999. In 2001, he entered the graduate school at the Electrical Engineering Department of the University of Tennessee, Knoxville. He was given a teaching assistantship in the same department.

Since Fall 2001, Ömer has been working in Wireless Communication Research Group (WCRG), where he will pursue his doctorate degree.